Stony Brook University

Using Biomechanics to Study Cell Behaviors

A Dissertation Presented

by

Chung-Chueh Chang

to

The Graduate School

in Partial Fulfillment of the

Requirements

for the Degree of

Doctor of Philosophy

in

Materials Science and Engineering

Stony Brook University

August 2012

Stony Brook University

The Graduate School

Chung-Chueh Chang

We, the dissertation committee for the above candidate for the

Doctor of Philosophy degree, hereby recommend

acceptance of this dissertation.

Dr. Miriam Rafailovich – Dissertation Advisor
Distinguished Professor of Department of Materials Science and Engineering
Stony Brook University

Dr. Vladimir Jurukovski - Chairperson of Defense
Adjunct Professor of Department of Materials Science and Engineering
Stony Brook University

Dr. Jonathan Sokolov
Professor of Department of Materials Science and Engineering
Stony Brook University

Marcia Simon
Professor of Department of Oral Biology and Pathology
Stony Brook University

This dissertation is accepted by the Graduate School

Charles Taber
Interim Dean of the Graduate School

Abstract of the Dissertation

Using Biomechanics to Study Cell Behaviors

by

Chung-Chueh Chang

Doctor of Philosophy

in

Materials Science and Engineering

Stony Brook University

2012

To develop stem cells based regenerative therapies, more efficient scaffolds are needed. Here we demonstrate how polymeric elastomer scaffolds can be used to induce differentiation of dental pulp stem cells (DPSCs) through surface interactions in the absence of chemical inducers. We show how these elastomers support DPSC proliferation and adhesion when plated directly on the uncoated polymer surfaces. Instead of physically or chemically crosslinking the polymers, we use the principal of entangled polymer surface confinement (EPSC) to continuously vary the substrate modulus and imprint patterns where only the underlying mechanics are varied while the surface chemistry and topography remains unchanged. The ability to continuously vary the mechanics and impose mechanical, topological, and chemical patterns independently provides a distinct advantage to these scaffolds relative to the hydrogel materials currently in use.

Using these elastomers, we demonstrated: (1) the principal of EPSC for PB films on Si substrates, and showed that the modulus decreased exponentially with increasing film thickness

(2) that EPSC could be used to generate substrates with relatively flat topography, but large differences in mechanical response, and (3) that, in the absence of chemical inducers (dexamethasone; Dex), DPSC are sensitive to differentially small changes in substrate mechanics continuously adjusting their cytoskeleton such that their modulus is always within a factor of 2.5 ($p<0.01$) of the substrate value.

Using a variety of complementary techniques, (SEM/EDX, GIXD, and qRT-PCR), we also found a critical value for the DPSC modulus above which odontogenesis occurred without Dex; Dex induced osteogenesis. Using confocal imaging with immunohistochemistry, we further determined that differentiation occurred in cells not in direct contact with the PB substrate, although cells removed from the mechanical stimulus, deposited $CaCO_3$, rather than hydroxyapatite. Finally, we probed the response of DPSC to mechanical heterogeneity by studying biomineralization on nanoscale and microscale patterns. We found that microscale patterns hindered biomineralization, even in the presence of Dex, while nanoscale patterns promoted biomineralization, even without Dex. Hence, it was not clear whether cells with different degree of differentiation could be co-cultured and self-assembled on the same substrate through mechanical templating.

Table of Contents

List of Figures

Chapter 1

Introduction

1.1 Overview of biomechanics

Living cells in the human body are constantly subjected to mechanical stimulations throughout life. These stresses and strains can arise from both the external environmental and internal physiological conditions [1]. It have also shown that many biological processes, such as growth, differentiation, migration, and even apotosis are affected by changes in cell shape and structural integrity [2, 3, 4]. Apart from mechanical stimulations which can affect cell mechanics, many chemicals are also known to increase or decrease the mechanical properties of living cells. For example, cytochalasin D and latrunculin B can disrupt the actin filament cytoskeleton and adversely affect the stiffness of cells [5]. Therefore, the mechanical properties of certain types of cells may potentially reflect the state of their cytoskeleton structure and health. This may be useful for possible applications in clinical diagnostics and even therapy for certain types of disease. In addition, it is well known that the mechanical properties of individual cells can determine the structural integrity of whole tissue arising from the mechanical interactions between cells and the surrounding extracellular matrix (ECM) [6], as well as mechanical loads exerted at the tissue level are transmitted to individual cells and can influence their physiological functions [7].

1.2 Overview of biomechanics in stem cell

Many tissue cells exert contractile forces that mechanically couples them to elastic matrices and that influence cell adhesion, cytoskeleton organization, and even cell differentiation. Recent work has demonstrated that mesenchymal stem cells (MSCs) cultured on polyacrylamide (PA) gels of varying stiffness show drastically different morphologies, and expression of early neurogenic, myogenic, and osteogenic key marker were found [8]. Those results indicate that stem cells extract the biophysical information from ECM and convert it to biochemical signals which further alter their cytoskeleton and gene and protein levels resulting in changes in cell shape, function, and differentiation.

The process of cells to detect and respond to the extracellular environment by extracting biophysical information which is then translated in altered gene expression and cellular behaviors is known as mechanotransduction. Two different regimes of mechanotransduction have been proposed: (a) passive or 'outside-in sensing, in which the cells detect the outsides forces which are transduced into the cell, and (b) active or 'inside-out sensing, in which the cell generates internal forces that allow response to extracellular environment [9]. In the case of stem cell study, the mechanotransduction process becomes very crucial since stem cells are very sensitive to small changes in extracellular environments, both mechanical and chemical, and differentiate accordingly to the cues they receive.

According to Engler et al [8], PA gels they used were overlaid with collagen to enhance cell adhesion. Furthermore, the mechanical properties of gels were controlled by altering the concentration of cross-linker. Although cell differentiation was shown to correlate with the

mechanical properties of the PA gels obtained from bulk measurements, the influence of coating collagen and altered concentrations of cross-linker on stem cells differentiation still remain unknown. To appropriately investigate the mechanotransduction process of stem cells, it is necessary that the stem cell differentiation is clearly modulated by the mechanical properties of the substrates not by chemical or combination of both. To overcome this problem, the substrates of varying mechanical properties need to be produced by only change the physical properties not chemical properties.

Chapter 2 focuses on how to prepare the substrates of varying mechanical properties by simply altering polymer film thickness, where only the changes in physical properties are involved. Chapter 2 also focuses on the differentiation pathways of the dental pulp stem cells (DPSCs regulated by the mechanics of the polymer films. Chapter 3 discusses the necessity of the presence of the induction agent, both mechanical and chemical. This issue was addressed by first culturing the DPSCs in different conditions where combinations of mechanical and chemical inducers were applied. After a fixed time, known to result in differentiation, the cells were transferred to substrates which did not provide any mechanical induction cues. Chapter 3 discusses the influence of mechanical heterogeneity on the adherence and differentiation of DPSC. I describe the methodology for forming micro and sub micron scale patterns using polymer self assembly techniques, and the physics for attenuation of the pattern at the sample surface.

1.3 References

[1] Lim C.T., Zhou E.H., Quek S.T. Journal of Biomechanics. 2006; 39: 195-216.

[2] Chen C.S., Mrksich M., Huang S., Whitesides G.M., Ingber D.E. Science. 1997; 276(5317): 1425-1428.

[3] Boudreau N., Bissell M.J. Current Opinion in Cell Biology. 1998; 10: 640-646.

[4] Schwartz M.A., Ginsberg M.H. Nature Cell Biology. 2002; 4: 65-68.

[5] Nagayama K., Nagano Y., Sato M., Matsumoto T. Journal of Biomechanics. 2006; 39(2): 293-301.

[6] Zahalak G.I., Wagenseil J.E., Wakatsuki T., Elson E.L. Biophysical Journal. 2000; 79(5): 2369-2381.

[7] Guilak F., Mow V.C. Journal of Biomechanics. 2000; 33(12): 1663-1673.

[8] Engler A.J., Sen S., Sweeney H.L, Discher D.E. Cell. 2006; 126: 677-689.

[9] Holle A.W., Engler A.J. Current Opinion in Biotechnology. 2011; 22: 648-654.

[10] Ingber D.E. Ann. Med. 2003; 35: 564-577.

[11] Lee G., Lim C.T. TRENDS in Biotechnology. 2006; 25(3): 111-118.

[12] Vliet K.J., Bao G., Sureah S. Acta Materialia. 2003; 51: 5881-5905.

[13] Lim, C.T., Zhou E.H., Li A., Vedula S.R.K., Fu H.X. Materials Science and Engineering C. 2006; 26: 1278-1288.

Chapter 2

Entangled polymer surface confinement, an alternative method to control dental pulp stem cells (DPSCs) differentiation in the absence of chemical mediators

2.1 Introduction

The cells can detect and respond to the extracellular environment by extracting biophysical information which is then translated in altered gene expression and cellular behavior- a process named mechanotransduction. Two different regimes of mechanotransduction have been proposed: (a) passive or 'outside-in' sensing, in which the cells detect outside forces which are transduced into the cell, and (b) active or 'inside-out' sensing, in which the cell generates internal forces that allow for response to the extracellular environment [14]. In the case of stem cells, the mechanotransduction process is very important *in vivo*. These cells are sensitive to small changes in the environment, both chemical and mechanical, and differentiate accordingly to the sum of the cues they receive. *In vitro*, however, it is very difficult to spontaneously differentiate stem cells without chemical induction factors.

Recently, it was shown that mesenchymal stem cells differentiation could be regulated by growth on collage coated polyacrylamide gels with different elasticity [15,16]. These studies indicated that the effect of the stiffness is related to the expression of non-muscle myosin II. This is consistent with other studies demonstrating that surface stiffness influence cell mechanics and their cytoskeleton [17,18,19] as well as with those demonstrating that the physical

characteristics of the extracellular matrix (ECM), such as elasticity, morphology, composition and structure, can affect the migration, proliferation and differentiation of stem cells [20,21, 22,23].

Undifferentiated mesenchymal stem cells isolated from dental pulp (dental pulp stem cells (DPSCs)) when grown in specific inducing media can differentiate and express markers of odontoblasts, osteoblasts, adipocytes or neuronal cells [24,25,26,27,28]. In addition, DPSCs have been shown to produce dentin when implanted in immuno-compromised mice [24,26,29]. cDNA microarray analyses show that DPSCs with dexamethasone (Dex), an active glucocorrticoid analog, in presence of inorganic phosphate and ascorbic acid results in the production of a mineralized calcified matrix with sparsely distributed condensed nodules containing high levels of calcium [24]. DPSCs are located in the relatively soft environment of the pulp and differentiate into odontoblasts which produce mineralized matrix-dentin. Changes in the pulp as result of tooth damage or bacterial infection can trigger its calcification of the pulp and effectively render the tooth dead. This transformation correlates with the influx of inflammatory cytokines and the change in the mechanical properties of the pulp [31,32]. Obviously changes in the chemical and physical properties of the environment include signal transduction events leading to differentiation.

The replacement and dealing of damaged tissues and organs is the central focus of regenerative medicine and the utilization of stem cells. Of concern is the control of their proliferation and proper differentiation after transplantation, where these cells require, or are likely to receive additional chemical stimuli that can affect both the transplanted stem cells and their surrounding tissue and lead to unpredictable results.

The use of materials whose mechanical properties can regulate or direct stem cell proliferation and differentiation [15,16] offers exciting applications. To appropriately investigate the processes of mechantransduction, it is necessary that the stem cell differentiation is clearly modulated by the mechanical properties of the substrates but not chemical or combination of both. Engler et al [15,16] used substrates made from polyacrylamide gels overlaid with collagen. In these experiments the mechanical properties were controlled by varying the acrylamide crosslinker and hence the cross-linking density. Although the mechanical properties of the collagen coating was not directly measured, cell differentiation was shown to correlate with the mechanical properties of the acrylamide gels obtained from bulk measurements, which were not sensitive to the actual moduli of the sample surface. In this model, the differences of moduli required to affect differentiation were larger (1kPa- 100kPa), and may have been much larger than the surface deviations. In addition, both chemical and mechanical induction of differentiation was used [16].

In order to accomplish differentiation in the absence of any chemical factors or coatings, we propose an alternative method to cross-link hydrogel scaffolds. It has been previously established that confinement of long chain entangled polymers near an interactive surface, can pin the chains to the surface, forming an effective “strangulated” gel, or a gel where the motion of the polymer is constrained by adding crosslinked points, where the statistical distance between crosslinks is small that the natural entanglement length of the polymer. It was shown that the influence of the confinement on the rheological properties of the films persisted for more than 10 polymer radii of gyration (Rg) from the surface [33,34]. Hence, through variation of the film thickness it was shown that the viscosity of the film can be changed by more than an order magnitude. We therefore postulated that the mechanical response of the films can also be

controlled simply by changing the film thickness of polymer on a surface which interacted favorably with the polymer. Here we demonstrate that this is indeed the case when long chain, entangled elastomers are used. Furthermore, we show that this method can be used to determine the functional form, which as expected is continuous and differential, of the change in modulus with film thickness, or distance from the interacting surface. This platform then allows us to ask several fundamental questions regarding stem cell response to changes in thee substrate mechanics which cannot otherwise be addressed in a hydrogel system.

In this study, we introduce the use of polybutadiene (PB), which is a biocompatible, synthetic rubber material similar to the natural rubber gutta-percha, material used in dentistry to fill root canals. PB can be synthesized in the monodisperse form, with high molecular weight chains, (Mw= 205K, Mw/Mn= 1.49) such that Rg= 135Å. It has been shown that when polyethylene-propylene (PEP) films are spun cast on hydrofluoric acid passivated Si substrates, complete wetting occurs when the film thickness exceeds Rg and annealing is performed in ultra-high vacuum (UHV) conditions, where the chains interact with the Si substrate [35,36]. Since PB is a rubber under ambient condition (Tg= -95˚C), the effect of surface interactions on PB films of varying thickness can be probed without the high temperature conditions described in the previous literature [34]. Furthermore, when annealed under these conditions, X-ray reflectivity in conjunction with atomic force microscopy, have shown that the films produced are extremely uniform with an RMS roughness less 6Å [36]. Hence PB provides the ideal substrate for probing only the effects of variable substrate mechanics, without any chemical or topographical variations, on biological systems where the operational temperate range is restricted to 37˚C. Here we described the use of specially processed PB films whose surface properties and thickness can be characterized with nanometer precision, to produce substrates

with controlled mechanical response, in order to investigate to what degree DPSC can sense the mechanics of the underlying substrates and determine whether a critical value exists for the modulus above which the cells will spontaneously differentiate.

2.2 Materials and methods

(a) Sample preparation

To prepare various thicknesses of PB spun-cast films, monodisperse polybutadiene (Mw= 205,800, Mw/Mn= 1.49; Scientific Polymer Products, Inc.) were dissolved in Toluene (certified A.C.S.; ACROS) at different concentrations (w/v). The polished silicon wafers (Wafer World Corporation, West Palm Beach, FL) used in this study were etched then spun-cast at 2,500 rpm onto HF-etched wafers to produce of PB films with thicknesses of 200, 500, 1500, 2000 and 3000Å as measured by ellipsometry. PB films were then annealed in the ultra-high vacuum oven at 10^{-8} torr at 150˚C for 24h to remove the residual solvent and further sterilize PB films for DPSC culture.

(b) Cell isolation and culture

Dental pulp stem cells (DPSCs) strain AX3 were isolated from the third molar teeth (IRB #20076778) as previously described [11] and were grown in α-MEM media (Invitrogen) supplemented with 10% fetal bovine serum, 200μM L-ascorbic acid 2-phosphate, 2mM L-glutamine, 100 units/ml penicillin/ 100μg/ml streptomycin, and 10mM β-glycerophosphate. As control, osteogenic induction of the DPSC was achieved by addition of 10^{-8}M Dex (Sigma-Aldrich). The cells were grown at 37˚C in a 5% CO2 cell culture incubator (Fischer Scientific).

(c) Cell plating and proliferation

DPSCs were harvested, counted and then plated on tissue culture polystyrene plastics (TCP) and PB films at a density of 5,000 cells cm^{-2}. For the study of cell proliferation, the cell number was determined on day 3, 5 and 7 using Hemacytometer (Hausser Scientific).

(d) Shear modulation force microscopy (SMFM)

The moduli of PB films and DPSCs cultured on PB films were measured by atomic force microscopy (AFM, Dimension 3000; Digital Instruments, Santa Barbara, CA) on shear modulation force microscopy mode. The experimental setup of the SMFM method is described in earlier articles [37,38]. Briefly, the AFM tip, applied to indent the surface, was laterally modulated and the mechanical response was fed into a lock-in amplifier and recorded. During the measurement, a normal indenting force of 25nN was exerted by the cantilever to induce a small oscillatory motion. The lateral deflection (response) amplitude of the cantilever was measured against the drive amplitude, both in mV, the response amplitude, therefore, being proportional to drive amplitude [39].

(e) Nanoinddentation

Instrumented indentation was performed using a nanoindenter (Micro Materials Nano Test) with diamond spherical indenters. Depth controlled indentations were performed with the maximum depth set from 35 to 60 nm depending on the sample, and represented no more than 30% of the total film thickness. A 5μm radius of curvature conical indenter was used on the film samples, and a 200μm radius spherical indenter used on the bulk sample. Film substrates were mounted with an epoxy adhesive to aluminum sample holders for testing. Load-displacement data was obtained using a constant loading and unloading rate of 1μN/s. Typical maximum loads reached were on the order of 50-200μN. A 5 second hold segment was taken at the

maximum displacement before unloading to take into account creep effects. On each sample, ten identical indentations were performed with a minimum spacing inverted of 50μm between successive indents to ensure no interaction between residual plastic deformations. To determine elastic modulus of the films, the slope (S) of the initial unloading data in conjunction with the spherical contact area is used in the conventional Oliver and Pharr method [40].

(f) Staining and laser scanning confocal microscopy (LSCM)

Immunocytochemistry was used to assess the state of the actin filaments, expression of osteocalcin and nuclear location. For that the DPSCs were washed with PBS, fixed with 3.7% formaldehyde solution for 15 minutes, permeabilized with 0.4% Triton X-100 in PBS and consequently incubated with 1:200 dilution of Alexa Flour 488 Phalloidin solution (Invitrogen, Carlsbad, CA) for actin fiber detection, 1:50 dilution of the rabbit anti-osteocalcin antibody (Santa Cruz) in 1% BSA/PBS solution for 1 hour at room temperature, followed by 30 minutes incubation with Texas red conjugated goat anti-rabbit secondary antibody (Santa Cruz). All incubations were followed by 0.05% Tween 20/PBS washes (2 x 5 minutes). The nuclei were visualized when needed by Propidium Iodide (Sigma Chemical Co., St. Louis, CA). Samples were analyzed and images captured using Leica TCS SP2 LSCM (Leica micro-system Inc., Bannockburn, IL).

(g) Scanning electron microscopy and energy dispersive X-ray (SEM/EDX)

Surface morphologies of PB films were characterized using scanning electron microscopy (SEM, LEO1550, LEO, German) at 20 kV acceleration voltage and 10 mm working distance. Samples were prepared by gently washing with DI water to remove soluble salts from media and air-drying for 1 day. Samples were sputter-coated with gold for 15s and loaded on

aluminum stubs for SEM imaging. The elemental compositions of deposits on PB films were determined by using Energy dispersive X-ray spectroscopy in conjunction with SEM.

(h) Grazing incidence X-ray diffraction (GIXD)

The crystal structures of deposits on PB films were characterized using synchrotron grazing incidence X-ray diffraction (GIXD) on beam-line X6B at the National Synchrotron Light Source at Brookhaven National Laboratory. Focused X-ray beam at 0.6525Å wavelength (spot size: 0.25 mm high, and 0.4 mm wide) was used to determine the structure of the deposits. In addition, the commercial synthetic hydroxyapatite (Product #574791; Sigma) was examined in GIXD geometry as a powder dusted on a blank PB substrate and in transmission in a glass capillary tube (1.0 mm diameter). Samples were mounted in air 150 mm from the detector screen. Grazing incidence diffraction patterns with incident angle 0-2˚ were recorded using an X-ray CCD detector (Princeton Instruments, Trenton, NJ) and calibrated using a standard Al_2O_3 powder plate.

(i) Real time- polymerase chain reaction (RT-PCR)

The gene expression levels of bone alkaline phosphatase (ALP) and osteocalcin (OCN) in DPSCs grown on PB films at various time points and up to 21 days of incubation were performed using gene specific primers (ALP- forward primer: 5'-GTACTGGCGAGACCAAGCGCAA-3' and reverse primer: 5'-ACCCCACACAGGTAGGCGGT-3'; OCN- forward primer: 5'-ATGAGAGCCCTCACACTCCTCG-3' and reverse primer: 5'-GTCAGCCAACTCGTCACAGTCC-3'). For the quantification SyBr Green RT-PCR kit (Sigma-Aldrich) and MJ Research DNA Engine Opticon PCR machine were used (Stony Brook

University DNA Sequencing Facility). The total RNA was isolated using RNeasy Mini Kit (Qiagen, Valencia, CA) according to the manufacturer's instructions. Random hexamers and Superscript II reverse transcriptase (Invitrogen, Carlsbad, CA) were used for cDNA synthesis.

2.3 Results and discussion

(a) Cell proliferation

In order to determine the biocompatibility of PB with DPSCs, and whether substrate mechanics influenced proliferation, the population doubling time of cells grown on PB films was compared to that of cells grown on TCP. PB films of two thickness were used: t= 200Å, which is slightly less than 2 Rg, where surface influences were expected to result large increase of the modulus relative to the bulk value obtained for the thicker film, t= 2000Å, or nearly 20 Rg where the influence of the substrate was expected to be minimal. The cells were counted at 3, 5 and 7 days after plating and confocal images of the cells, stained with Alexa Fluor 488 Phalloidin for actin and propidium iodide for nuclear localization, were taken at day 7. As shown in Figure 2.1, the doubling time of the cells on the thin PB substrate (50.1±1.7 h) is close to the value on TCP (41.5±4.2 h, $p<0.05$), indicating that the harder PB surface supported cell adhesion and proliferation similar to TCP, without the need for additional surface modification. On the thick PB substrate the doubling time increases dramatically (76.5±2.5 h, $p<0.005$). Since the surface chemistry of the substrate was not altered, these results indicate that the cells are sensitive to changes in substrate mechanics and are adversely affected by the decrease in modulus. Confocal images of the cultures at day 7 (Figure 2.2), show that the cells grown on the thin PB substrate are well extended with organized actin fibers, similar to those on TCP, while the cells grown on thick PB show less organized actin cytoskeleton and morphology. Similar results were reported

by Ghosh et al [41] who observed that the fibroblasts plated on harder hyaluronic acid (HA) cross-linked hydrogel substrates had more extended actin filaments and exerted larger traction forces compared to cells plated on softer cross-linked HA substrates. Since cell division is in part regulated by the ability of cells to exert large traction forces [41], the increased doubling time on the softer PB substrate may be due to the inability of the cells to exert adequate traction forces.

(b) Mechanics of surfaces and DPSCs plated on surfaces

In order to determine the extent to which the hardness of the films changes with film thickness, SMFM and the nanoindentation technique were used to measure the moduli. As shown in Figure 2.3(a), the moduli measured by the two methods were in good agreement on dry samples. Cell mechanics could be measured only by the indentation using the SMFM liquid cell setup method; this method was used for all subsequent analyses. As shown in Figure 2.3(b) the values obtained for the PB films in cell culture media were proportional to those measured when they were dry. This result indicates that the moduli are stable throughout the incubation time with the cells at least for 14 days, and that PB, as expected, is not hydrated nor degraded by components present in media. The moduli of PB films and DPSCs on these films are plotted in Figure 2.4(a) as a function of film thickness. It is apparent that both the moduli of the films and that of the cells follow a continuous decreasing exponential function with increasing film thickness. The decrease in viscosity with film thickness first reported by Zheng et al [34] had a similar functional form, except that the decay length was somewhat larger, 10Rg, whereas for PB is 8 Rg. Since the propagation of the surface interactions into the interior of the polymer film was shown to be due to entanglements, this difference can be explained by differences in the entanglement length between the two polymers, and the strength of the polymer/substrate

interaction. The moduli of the clls as a function of the moduli of the underlying substrate obey a linear relationship with a slope of 0.392 (Figure 4(a)- inset). This indicates that the modulus of the cells is also continuously differentiable with changes in the modulus of the films, with a fixed proportionality constant. Hence, even though it was previously demonstrated that cells are capable of adjusting their cytoskeletal components in response to changes in substrate mechanics [42, 43], the precise functional form or the degree of sensitivity had not been previously demonstrated.

Also, Figure 2.4(a) presents the modulus measured for DPSC cultured on TCP together with the modulus of the TCP surface. Even though the modulus of TCP is higher than that of the thinnest PB film studied, the moduli of the cells are nearly half of those of the cells on PB. This illustrates that despite the ability of the cells to sense surface mechanics, other factors, relating to chemistry of the surface, are also important. Hence it is difficult to predict the ability of a material to induce differentiation based on extrapolations of the mechanical properties alone.

Ba et al [44] and Meng et al [45] have studied the effects of substrate and external magnetic field on the biomineralization of murine osteoblasts after four weeks, and observed that it was consistently accompanied by an increase in the moduli of the cells within the first week after induction by the field and the mechanical properties of the extracellular matrix. Therefore the moduli of the cells on both PB and TCP as a function of incubation time were measured and correlations were made between the moduli at early time points and the deposition of biomineralizaed products after 21 days. The moduli of cells plated on thin PB films (200Å) and thick PB films (2000Å) and TCP, measured at days 4, 7, 11 and 14 are plotted in Figure 2.4(b). The DPSCs were grown either without Dex (non-inducing media (-)) or with Dex (inducing media (+)). The moduli on all substrates were similar after four days of incubation, with

differences becoming apparent at day 7. In the case of TCP, Gronthos et al [26] have shown that in the presence of Dex, cultures of DPSC accumulate calcified deposits after six weeks and express markers of osteogenesis and odontogenesis. As shown in Figure 2.4(b) the moduli of cells grown on TCP with Dex are larger by 50% ($p<0.01$) than those incubated without Dex, which is consistent with the observations for murine osteoblasts [44, 45]. In the case of the thick PB substrate, the moduli of the cells at day 7 are roughly 60% smaller than the moduli of the cells plated on TCP, which is expected, since the modulus of TCP, shown in Figure 2.4(a), is more than two orders of magnitude higher than that of PB. Addition of Dex to the incubation media of the thick PB samples resulted in an increase in the moduli of the cells by nearly a factor of three, to a value which is similar to that of the cells plated on TCP in presence of Dex. In this case, Dex rather than the modulus of the substrate appears to determine the moduli of the cells. It is interesting to note that in the case of the cells grown on thin PB without Dex, the moduli of the cells is 40% ($p<0.01$) higher than that for the cells on TCP, despite the fact that the modulus of the substrate is more than an order of magnitude lower. This illustrates the fact that the chemistry of the surface might be the more important factor in determination of the modulus, when the chemical induction factor, Dex, is absent. Comparing the cell's moduli with that of the PB substrates shows that a decrease by a factor of four in substrate modulus results in almost two-fold increase in the moduli of the cells, emphasizing the role of substrate mechanics surfaces with identical surface chemistry. These results are consistent with the observed morphology of the actin fibers of the cells on day 7 (Figure 2.2). Namely in the absence of Dex, when cells have higher moduli cells have well organized actin fibers and well extended cell morphology.

Dex presence in the media when cells were grown on thin PB results in an additional increase in the cell modulus by nearly 30% in compared to the ones grown in absence of Dex,

indicating a synergistic or additive effect when mechanical and chemical induction are combined. The same figure shows that under all growth conditions the modulus reaches a plateau at day 7 and the increases between day 7 and 14 are not significant.

(c) Characterization of the biomineralization deposits

In order to determine whether the increase in modulus of DPSCs correlated with eventual biomineralization after four weeks, as previously reported for the osteoblasts [44, 45], the DPSC were grown on the thin (200Å) and thick (2000Å) PB substrates for 28 days in presence or absence of Dex. As shown in Figure 2.5, the SEM images show large amounts of biomineralized deposits on the samples of cells grown on thin PB either with or without Dex, and on cells grown on thick PB in the presence of Dex. No deposits were observed on thick PB substrates in absence of Dex. These results indicate that mechanics alone can induce DPSCs to form biomineralized matrix when plated on thin PB surfaces. In agreement with previously published data, no biomineralization was observed in cultures grown on TCP in media without Dex [11] (data not shown). EDX spectrums of the deposits (Figure 2.5(c), (f)), confirm that the mineral deposits are all calcium phosphates. Comparing these results and the increase in cell moduli at day 7 (Figure 2.4(b)) it is noticeable that only the samples that have increased cell moduli were shown to biomineralize (Figure 2.5(a), (c), (d)) which might indicate that in the case of DPSC the early increase in modulus at day 7 could serve as an indicator of eventual biomineralization.

In order to determine whether critical value of the substrate mechanics exists above which biomineralization is induced, DPSCs were grown on PB films with varying thicknesses ranging from 200 to 3000Å in absence or presence of Dex for 21 days. Biomineralized deposits were observed on all surfaces grown in inducing media (Figure 2.6(f)-2.6(j)), indicating that

significant deposition can be observed as early as 21 days in chemically induced cells. Biomineralized deposition cells grown without Dex could only be seen on substrates thinner than 1500Å (Figure 2.6(a)-(e)), corresponding to a critical modulus cutoff of 2.5 MPa (Figure 2.4(a)). EDX analyses confirmed that these deposits were calcium phosphates (Figure 2.4(k), (l)).

The uniformity of the deposits across the sample and their crystal structure were evaluated by grazing incidence X-ray diffraction analyses. The data are shown in Figure 2.7, together with spectra of a hydroxyapatite control sample. Two discernible peaks were observed on all surfaces from Dex containing cultures and on surfaces with PB thicknesses below 1500Å from Dex-free cultures. These peaks correspond to [002] and the combined [211] and [112] reflections of hydroxyapatite, which is the main component of osseous (bone) tissue. No peaks were observed on the surfaces which did not show presence of calcium phosphate on the SEM images (Figure 2.6(c)-(e)), leading to conclusion that no deposition, either crystalline or amorphous had occurred.

(d) Gene and protein expression

Expression of two markers of osteogenic differentiation, alkaline phosphatase (ALP) and osteocalcin (OCN), by DPSCs was characterized using Real Time-PCR. RNA was isolated from DPSCs grown on thin and thick PB, in absence or presence of Dex, at different time points, up to day 21 of growth. As shown in Figure 2.8, no significant differences in the expression of ALP and OCN mRNA were observed between day 1 and day7 for all samples. Even though an increase in the expression of ALP mRNA was observed for all samples on day 14 (Figure 2.8(a)), the increase was nearly twice as large in the samples that were grown on thin PB without Dex and both PB samples grown in the presence of Dex in good correlation with the samples shown

to biomineralize (Figure 2.5). It appears that on thick PB the expression of ALP reaches a plateau after day 14 since no significant differences were observed in the samples with or without Dex. On the other hand, the expression of ALP appeared transient in cultures grown on thin PB with highest expression levels at day 14 and slight reduction at day 21. Still, the reduced ALP expression levels at day 21 in absence of Dex are higher in the thin PB samples compared to the ALP expression in the thick PB samples.

Similar to ALP, the OCN mRNA expression did not increase in any of the DPSC samples until day 14 (Figure 2.8(b)). By day 14 its expression increased 2-3 fold in each of the cultures that biomineralized (thin PB with or without Dex and thick PB with Dex); no significant increase was detected in cells grown on thick PB in the absence of Dex. At day 21, the samples containing Dex showed increased OCN expression for an additional 2.5 fold and those without Dex showed modest but significant increase. In absence of Dex the expression of OCN was still two fold higher in the samples grown on thin PB compared to that of thick PB. In addition the increase in OCN expression are in good agreement with the increase in cell moduli which are higher in the induced thin (200Å) PB samples at days 7-21 (Figure 2.4(b)), and suggests possible synergistic effects of chemical and mechanical cues. The similar increase in OCN level observed for cells grown on thin (200Å) PB samples in the absence of Dex might indicate that the up-regulation of the OCN, a late stage osteogenic marker, might be somewhat delayed since the DPSCs are only mechanically induced. These results may indicate that the OCN gene expression is regulated by two separate signaling pathways, one influenced by the mechanical pull of the cell, probably through focal adhesion points; and the other induced by Dex receptor mediated signaling events. The Dex signaling is complex in that its effects on signaling events

and ultimately gene expression vary with cell type and stage of cell growth and differentiation [46, 47] and requires further investigation in the case of DPSCs and their differentiation patterns.

(e) Confocal microscopy and immunofluorescent staining

Confocal microscopy images of the cells after 21 days of incubation, where actin fibers are stained with Alexa Fluor 488 Phalloidin (green), and the nuclei with propidium iodide (red), are shown in Figure 2.9, together with images for cells cultured on TCP. On TCP, the cells which were cultured in absence of Dex and did not show biomineralization (did not differentiate), have a different morphology than those which were grown in the media containing Dex and showed biomineralization (differentiation). The cells which were grown in presence of Dex and have differentiated, are not well organized, nor have extended actin fibers, and many have rounded appearance. A similar variation is observed between the cells cultured with and without Dex on the thick PB sample, except in this case, in absence of Dex the cell organization was not as good as in the TCP control, probably due to the influence of the substrate mechanics on the organization and distribution of the actin fibers. The largest difference was seen for cells cultured on the thin PB samples. The cells which were induced to biomineralize by chemical cues (Dex) have the same rounded appearance as the cells grown on TCP or thick PB, whereas the cells which were induced only by mechanical cues, have a more extended appearance, with small nodules of biomineralized material, but did not reach confluence as in the case of TCP. These results indicate that the type of induction (chemical vs. mechanical) may result in activation of different signaling pathways that lead to biomineralization.

Immunocytochemistry was used to measure the expression of OCN in different layers of the confluent cell cultures and to determine if the mechanical stimulus induces OCN expression

only in cells that are in direct contact with the surface. DPSCs grown for 21 days on thin and thick surfaces were stained with OCN specific antibody and were imaged using LSCM in z-axis slices at 0, 10, and 20μm from the surface (Figure 2.10). It is clear that OCN is expressed in all layers. In addition, no significant differences in its expression were detected among the three layers shown. In further attempt to characterize the relative amounts of OCN protein at various time points of incubation and surface contact, the intensities of OCN staining were analyzed by Image J (Figure 2.11). This analysis showed that the OCN gene expression and the amount of OCN protein closely correlate and follow the same overall pattern: in presence of Dex, OCN was observed on both thin and thick PB films and increased at days 14 and 21 regardless of cell-surface contact (Figure 2.8 and 2.11). In the absence of Dex, OCN was only detected in the cells grown on thin PB film and also increased over the 14-21 day interval regardless of cell-surface contact (Figure 2.8 and 2.11). Up-regulation of OCN protein was observed by day 14 on the cells grown on the thin PB sample, with and without Dex, with the largest increase at day 21 visible mostly on the cells incubated with Dex followed by the cells grown on thin PB. On the thick PB, no OCN is detected for cells at any time point in the absence of Dex, and significant expression is also observed at day 21 for the cells cultured in the presence of Dex. The presence of OCN in all layers examined are not surprising for the Dex induced cells, however, it was unexpected for the cells where differentiation was induced solely by the mechanical properties of the substrates; cells that are not in direct contact with the substrates express the differentiation marker to similar extent. This outcome can be result of several possible scenarios: the cells in direct contact with the substrate secrete cytokines which in turn induce differentiation of the upper cell layers; the modulus of the cells in direct contact with the substrate influences the

modulus of the cells in the upper layers in a similar manner as that of the thin PB; or both mechanisms may act in conjunction on the upper layer of cells.

2.4 Conclusions

The present study has shown that DPSC can be cultured on uncoated PB elastomeric polymer substrates. The modulus of elastomeric polymers is known to vary with film thickness, and this principle was used to generate substrates where only the mechanical properties are varied without any additional chemical modification or additives. Using SMFM, it was found that cells plated on these substrates adjust their moduli in a continuously differential form to follow the changes of the mechanics of the substrates. Using SEM in combination with EDX and GIXD, it was demonstrated that a critical value for the modulus of 2.5 MPa, corresponding to a film thickness of 1500Å, exists above which the cells were induced to produce crystalline hydroxyapatite biomineralized deposits, without addition of Dex as induction factor, as shown for all samples grown on thin PB. RT-PCR analyses of gene expression confirmed that the deposition was correlated with up-regulation of OCN and ALP, indicating activation of osteogenic differentiation pathways. The lack of differentiation in the absence of Dex observed for cell cultured on TCP, regardless of the much thicker substrate modulus than the thin PB, underscores the fact that mechanical cues alone are not a sufficient condition to induce differentiation. Cells differentiated by mechanical induction alone versus cells induced by chemical factors may express differentiation markers at different times. However, in all cases, a synergy was observed when DPSCs were induced by both mechanisms simultaneously. Immunofluorescent staining for OCN protein in expression was consistent with the gene expression of this differentiation marker in RT-PCR analyses. Spatially resolved images of the distribution of the OCN presence indicated that direct contact with the substrate was not

necessary for cells induced only by mechanical cues at the surface, emphasizing the need for further investigation on how substrate mechanics triggers additional pathways that lead to differentiation.

2.5 References

[14] Holle AW, Engler AJ. Current Opinion in Biotechnology 2011; 22: 648-654.

[15] Engler AJ, Sen S, Sweeney HL, Discher DE. Cell 2006; 126: 677-689.

[16] Engler AJ, Sweeney HL, Discher DE, Schwarzbauer JE. J. Musculoskelet Neuronal Interact 2007; 7(4): 335.

[17] Discher DE, Janmey P, Wang YL. Science 2005; 310: 1139-1143.

[18] Rehfeldt F, Engler AJ, Eckhardt A, Ahmed F, Discher DE. Advanced Drug Delivery Reviews 2007; 59: 1329-1339.

[19] Yeung T, Georges PC, Flanagan LA, Marg B, Ortiz M, Zahir N, Ming W, Weaver V, Janmey PA. Cell Motility and the Cytoskeleton 2005; 60: 24-34.

[20] Sen S, Engler AJ, Discher DE. Cellular and Molecular Bioengineering 2009; 2(1): 39-48.

[21] Reilly GC, Engler AJ. J. Biomechanics 2010; 43: 55-62.

[22] Holle AW, Engler AJ. Nature Materials 2010; 9: 4-6.

[23] Tse JR, Engler AJ. PLos ONE 2011; 6(1): e15978.

[24] Gronthos S, Mankani M, Brahim J, Robey PG, Shi S. Proc. Natl. Acad. Sci. 2009; 97(25): 13625-13630.

[25] Almushayt A, Narayanan K, Zaki AE, George A. Gene Therapy 2006; 13: 611-620.

[26] Gronthos S, Brahim J, Li W, Fisher LW, Cherman N, Boyde A, DenBesten P, Robey PG, Shi S. J. Dental Research 2002; 81(8): 531-535.

[27] Miura M, Gronthos S, Zhao M, Lu B, Fischer LW, Robey PG, Shi S. Proc. Natl. Acad. Sci. 2003; 100(10): 5807-5812.

[28] Nosrat IV, Smith CA, Mullally P, Olson L, Nosrat CA. European Journal of Neuroscience 2004; 19: 2388-2398.

[29] Batouli S, Miura M, Brahim J, Tsutsui TW, Fischer LW, Gronthos S, Robey PG, Shi S. J. Dental Research 2003; 82(12): 976-981.

[30] Shi S, Robey PG, Gronthos S. Bone 2001; 29(6): 531-539.

[31] Cooper PR, Takahashi Y, Graham LW, Simon S, Imazato S, Smith AJ. J. Dent. 2010; 38: 687-697.

[32] Goldberg M, Farges JC, Lacerd-Pinheiro S, et al. Pharmacol Res. 2008; 58: 137-147.

[33] Li C, Koga T, Li C, Jiang J, Sharma S, Narayanan S, Lurio LB, Hu X, Jiao X, Sinha SK, Billet S, Sosnowik D, Kim H, Sokolov JC, Rafailovich M. Macromolecules 2005; 38: 5144-5151.

[34] Zheng X, Rafailovich M, Sokolov J, Strzhemechny Y, Schwarz SA, Sauer BB, Rubinstein M. Physical Review Letters 1997; 79(2): 241-244.

[35] Zhao W, Rafailovich M, Sokolov J, Fetters LJ, Plano R, Sanyal MK, Sinha SK, Sauer BB. Physical Review Letters 1993; 70(10): 1453-1456.

[36] Tolan M, Seeck OH, Schlomka JP, Press W, Wang J, Sinha SK, Li Z, Rafailovich M, Sokolov J. Physical Review Letters 1998; 81(13): 2731-2734.

[37] Ge S, Pu Y, Zhang W, Rafailovich M, Sokolov J. Physical Review Letters 2000; 85(11): 2340-2343.

[38] Pu Y, Ge S, Rafailovich M, Sokolov J, Duan Y, Pearce E, Zaitsev V, Schwarz S. Langmuir 2001; 17: 5865-5871.

[39] Koo J, Rafailovich M, Medved L, Tsurupa G, Kudryk BJ, Liu Y, Galanakis DK. J. Thromb Haemost 2010; 8: 2727-2735.

[40] Oliver WC, Pharr GM. J. Materials Res. 1992; 7(6): 1564-1583.

[41] Ghosh K, Pan Z, Guan E, Ge S, Liu Y, Nakamura T, Ren XD, Rafailovich M, Clark RAF. Biomaterials 2007; 28: 671-679.

[42] Ingber DE, Heidemann SR, Lamoureux P, Buxbaum RE. J. Applied Physiology 2000; 89: 1663-1678.

[43] Yeung T, Georges PC, Flanagan LA, Marg B, Ortiz M, Funaki M, Zahir N, Ming W, Weaver V, Janmey PA. Cell Motility and the Cytoskeleton 2005; 60: 24-34.

[44] Ba X, Hadjiargyrou M, DiMasi E, Meng Y, Simon M, Tan Z, Rafailovich M. Biomaterials 2011; 32: 7831-7838.

[45] Meng Y, Qin Y, Dimasi E, Ba X, Rafailovich M, Pernodet N. Tissue Engineering: Part A 2009; 15(2): 355-366.

[46] Canalis E. J. Clinical Endocrinology and Metabolism 81: 3441-3447.

[47] Mei-Fway I, Hiroshi K, Hideaki S, Junko N, Toshitsugu S, Kazuo Chihara. J. Endocrinology 2005; 185: 131-138.

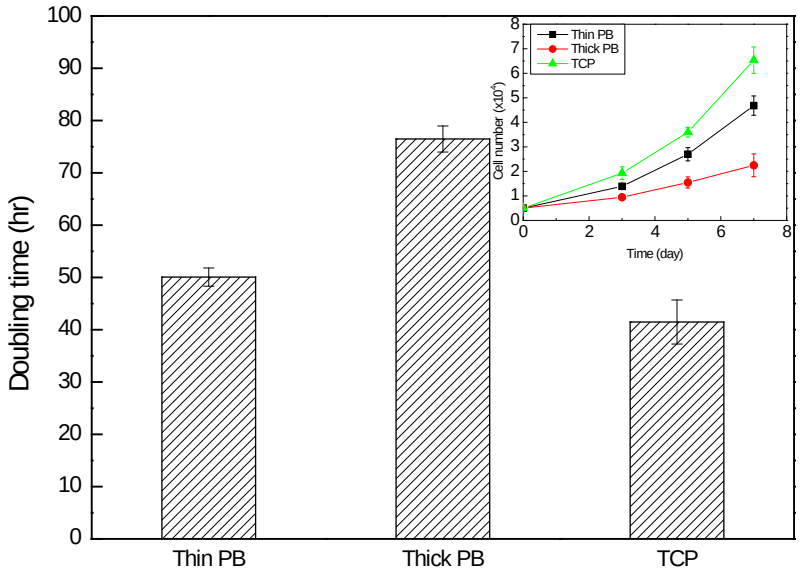

Figure 2.1 Cell proliferation and doubling time. Correlation of the doibling time and cell proliferation (inset) of DPSCs grown on thin (200Å) and thick (2000Å) PB with TCP as control.

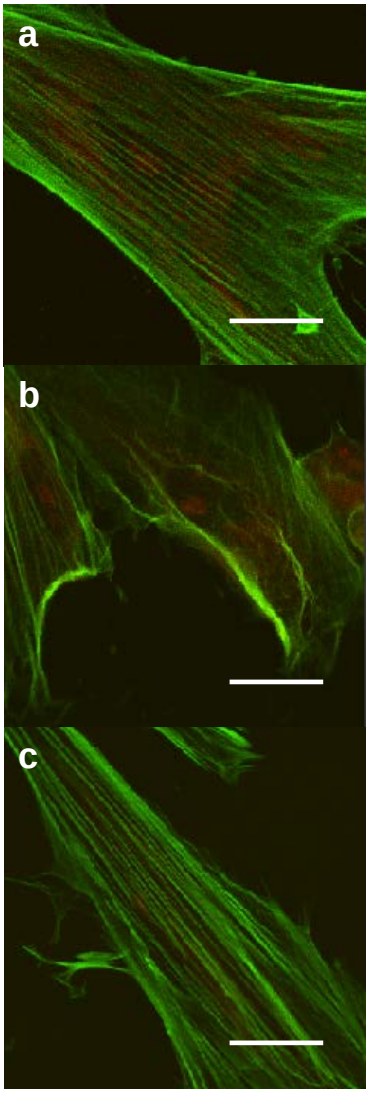

Figure 2.2 Actin filament distribution and cell morphology. The confocal images of DPSCs grown for 7 days on (a) thin (200Å) PB, (b) thick (2000Å) PB, and (c) TCP reveal the arrangement of actin filaments and cell morphology on different substrates. Scale bar= 25µm.

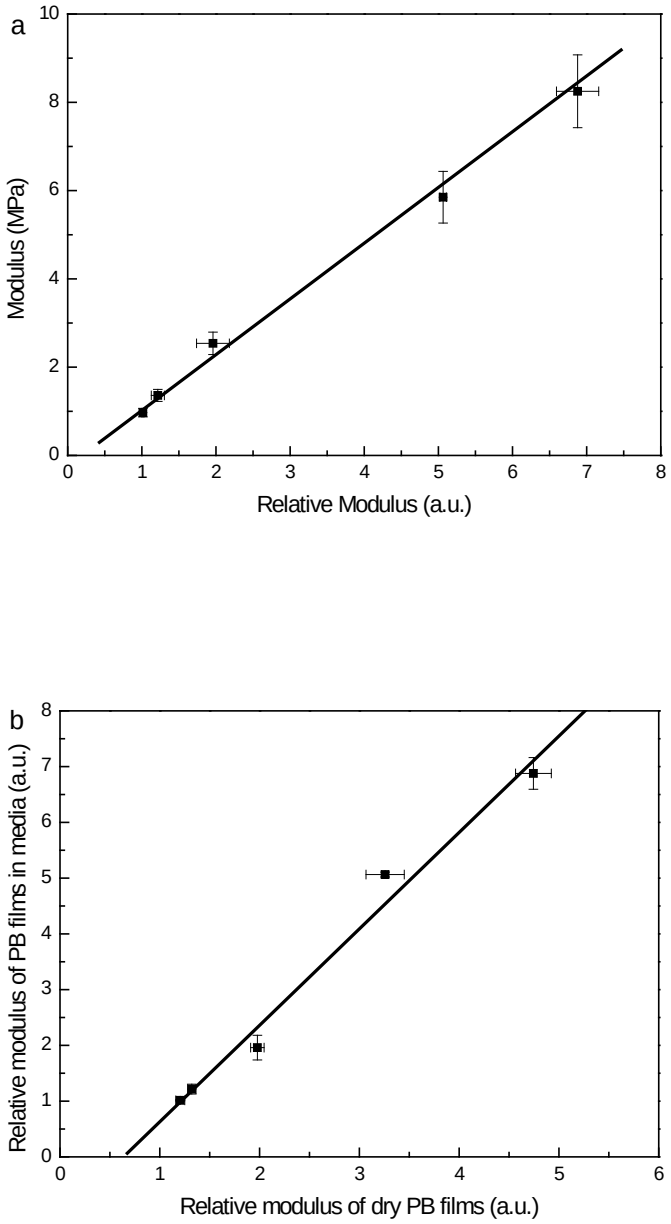

Figure 2.3 PB film moduli. (a) Shear modulation force microscopy and nanoindentation measurements of the moduli of PB films with thickness from 200 to 3000Å showing good agreement of results from both techniques. (b) The moduli of dry PB films and those in media are plotted showing no hydration or degradation of PB films in media.

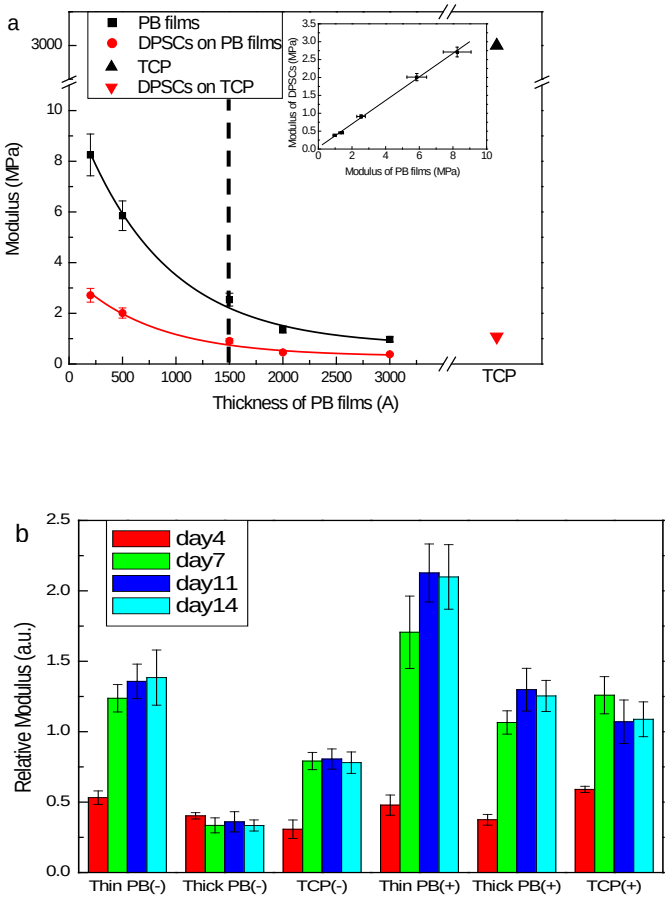

Figure 2.4 The correlation of the moduli of PB films and DPSCs. (a) Both PB and DPSCs follow a continuous decreasing exponential function with increasing film thickness. The inset shows a linear relationship of the moduli of the cells as a function of the moduli of the underlying substrates. (b) The moduli of the DPSCs grown with and without Dex on thin (200Å) and thick (2000Å) PB and TCP as the function of time.

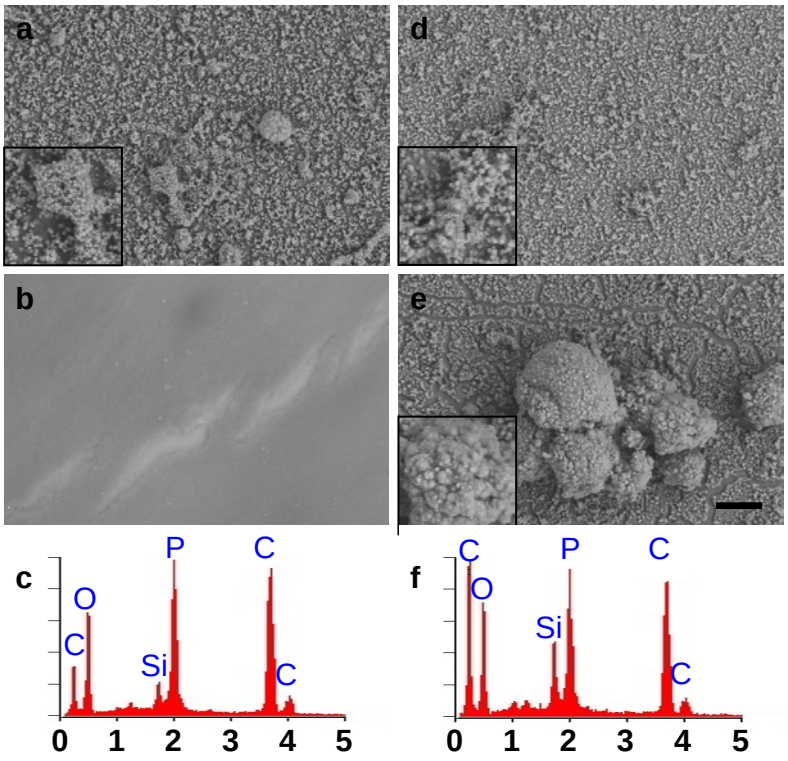

Figure 2.5 SEM images of DPSCs on (a, d) thin (200Å) and (b, e) thick (2000Å) PB films at day 28 without and with Dex, respectively. (c, f) EDX spectra of deposited minerals indicate that deposits are calcium phosphates. Scale bar= 15µm.

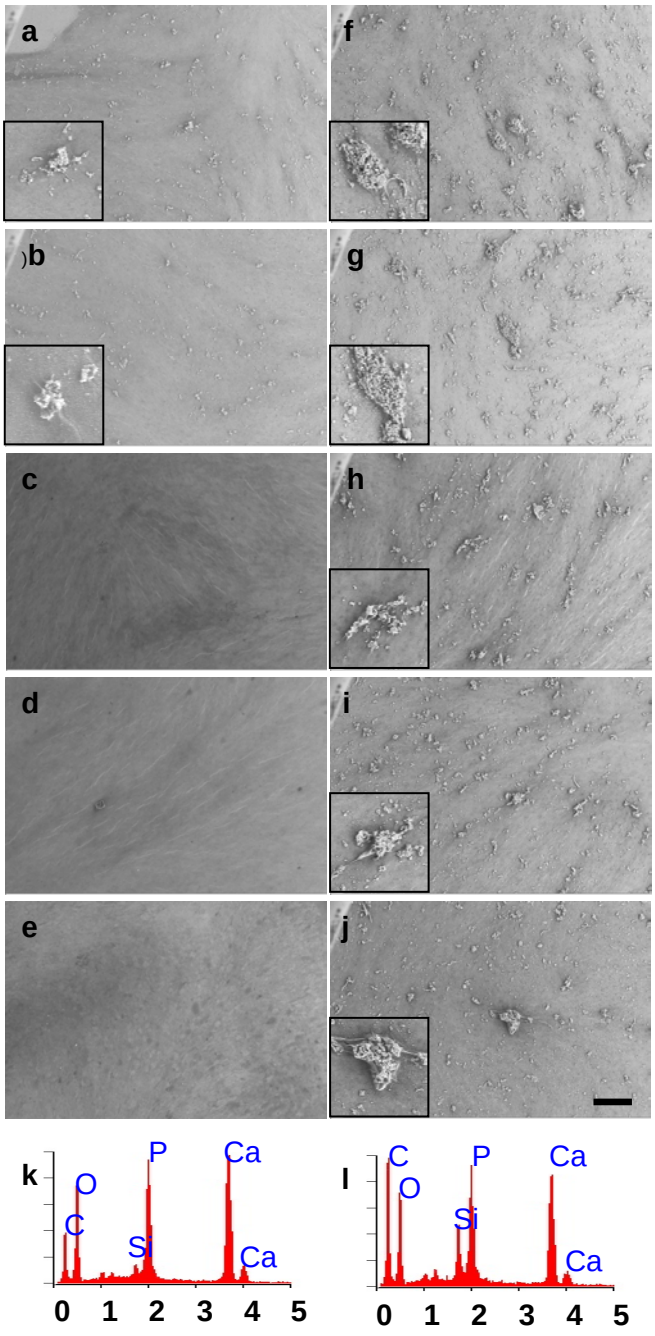

Figure 2.6 SEM images od DPSCs grown on PB films with thicknesses of (a, f) 200Å, (b, g) 500Å, (c, h) 1500Å, (d, i) 2000Å, and (e, j) 3000Å at day 21 without and with Dex, respectively. (k, l) EDX spectra of deposited minerals indicate that deposits are calcium phosphates. Scale bar= 25µm.

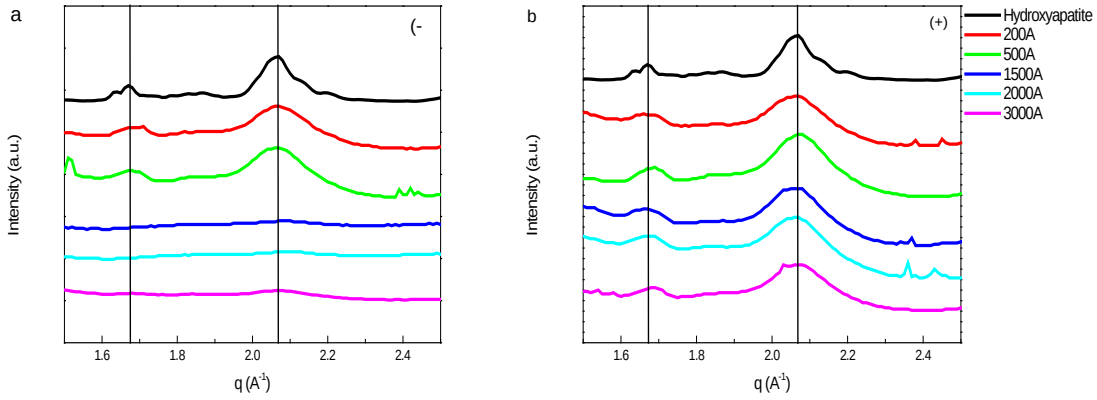

Figure 2.7 Synchrotron GIXD spectra of mineralized deposits on PB films with varying thickness (a) without Dex and (b) with Dex.

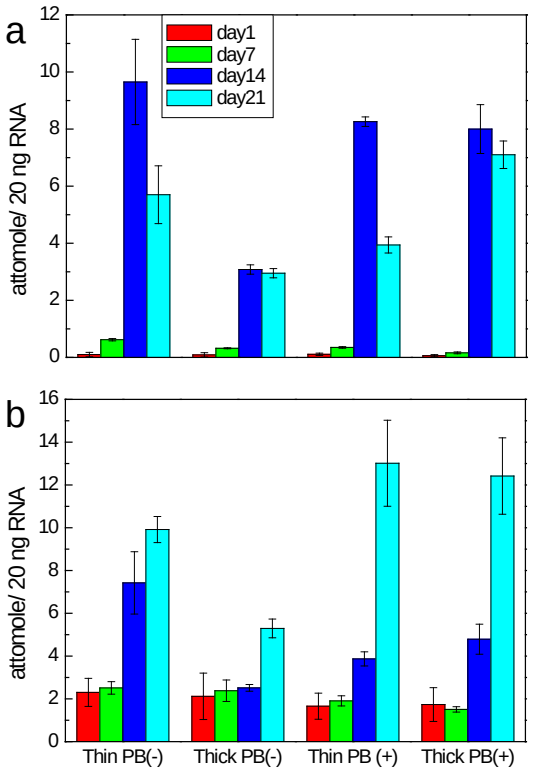

Figure 2.8 RT-PCR analyses of the (a) ALP and (b) OCN gene expression in DPSCs different growing conditions at day 21.

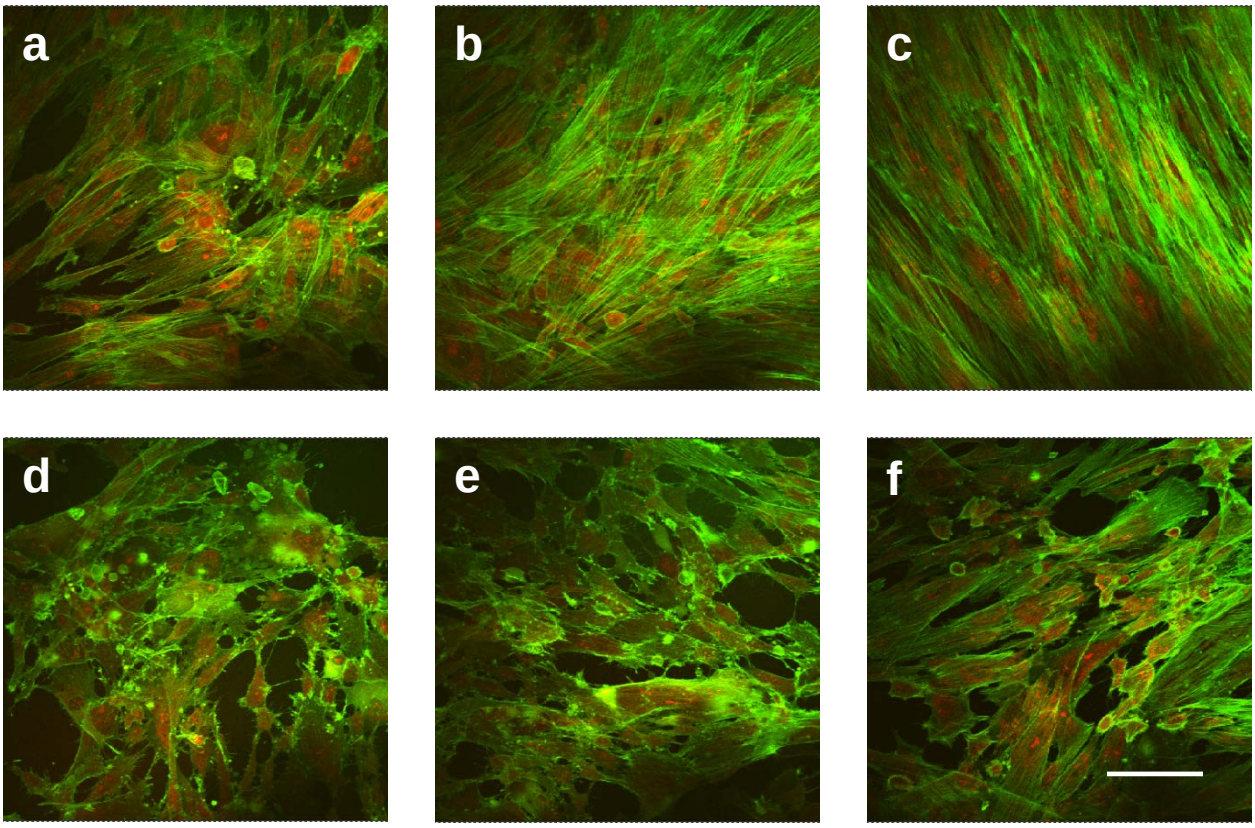

Figure 2.9 Confocal images of cell morphology and organization of DPSCs grown on (a, d) thin (200Å), (b, e) thick (2000Å) PB, and (c, f) TCP at day 21 without and with Dex, respectively.

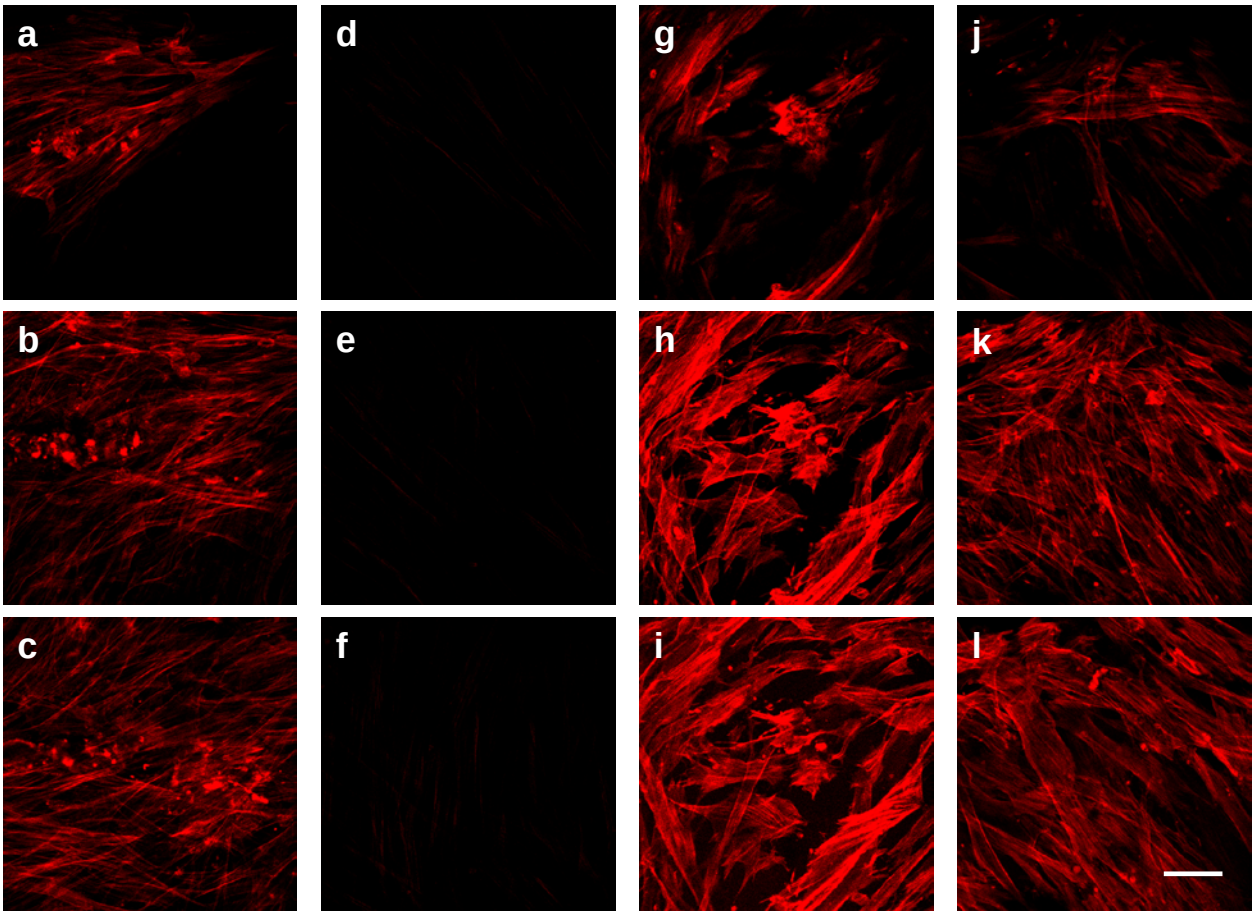

Figure 2.10 Confocal images of z-axis slices of DPSCs at 20, 10 and 0µm from the PB surfaces for OCN protein expression at day 21. The top, middle and bottom layers of DPSCs grown in absence of Dex on (a, b, c) thin (200Å) and (d, e, f) thick (2000Å) PB compared to DPSCs grown in presence of Dex on (g, h, i) thin and (j, k, l) thick PB. Scale bar= 50µm.

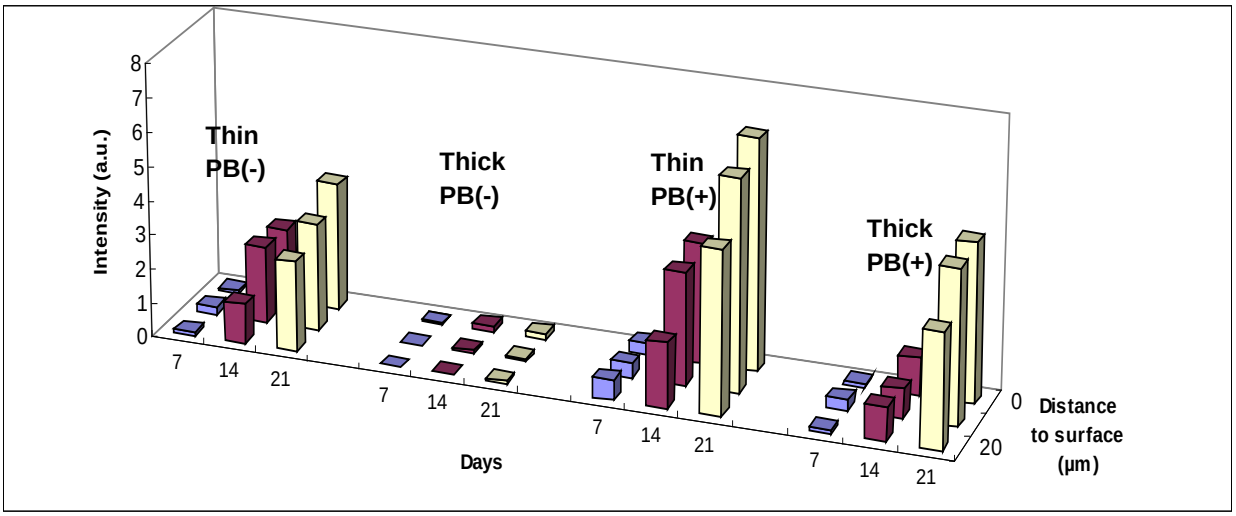

Figure 2.11 Quantification of fluorescence intensities of OCN protein expression of DPSCs at 20, 10 and 0μm from the PB surfaces up to day 21.

Chapter 3

The effects of mechanical inducer on dental pulp stem cells (DPSCs) biomineralization

3.1 The necessity of mechanical inducer on DPSCs biomineralization

It has been shown that DPSCs can be induced to produce biomineralized calcium phosphate deposits using mechanical and chemical cues (thin PB and Dexamethasone (Dex)). In addition, immunofluorescent staining analyses indicate that direct contact of cells with the surface (thin PB) originally providing the mechanical cue is not necessary for the differentiation of the overlying cell layers. This result opens up an interesting and important question. Are mechanical or chemical cues necessary to maintain DPSCs producing biomineralized deposits once DPSCs have been induced to differentiate? To answer the question of whether the induced cells maintain phenotype and are "educated", DPSCs were cultured on thin and thick PB and TCP with and without Dex. After a 21 days incubation, cells were trypsinized and re-plated on thick PB with and without Dex; growth on thick PB in the absence of Dex does not induce differentiation. The experimental scheme is shown in Figure 3.1.

First, using replicate cultures, DPSC function was assessed at 21 day post-induction. Confocal microscopy was used to visualize actin fibers stained with Alexa Fluor 488 Phalloidin (green), and nuclei stained with propidium iodide (red). As shown in Figure 3.2, are similar to previous studies on TCP, the cells which were cultured in absence of Dex have a different morphology than those which were grown in the media containing Dex. The cells which were

grown in presence of Dex have differentiated, are not well organized, do not have extended actin fibers, and many have a rounded appearance. A similar variation is observed between the cells cultured with and without Dex on the thick PB sample. The largest difference was seen for cells cultured on the thin PB samples. The cells which were induced to biomineralize by chemical cues (Dex) have the same rounded appearance as the cells grown on TCP or thick PB, whereas the cells which were induced only by mechanical cues, have a more extended appearance but did not reach confluence as in the case of TCP. Laser scanning confocal microscopy (LSCM), scanning electron microscopy and energy dispersive X-ray (SEM/EDX) were employed to investigate DPSCs biomineralization. The SEM images (Figure 3.3) show biomineralized deposits on the samples of cells grown on thin PB either with or without Dex, and on cells grown on thick PB in the presence of Dex. No deposits were observed on thick PB substrates in absence of Dex. These results are in agreement with previous study and EDX spectrums of the deposits (Figure 3.3(c), (f)) confirm that the mineral deposits are all calcium phosphates. The results confirm that DPSCs can be induced by surface mechanics (thin PB) and chemical inducer (Dex) to produce calcium phosphate deposits.

Replicate cultures generated by transfer of induced cells to thick PB were analyzed after another 21 day incubation and analyzed to determine whether DPSCs were “educated” and maintained their induced capacity for biomineralization. As shown in Figure 3.4, confocal images show no significant difference in cell morphology amongst cells preconditioned by prior growth on different surfaces or different exposures to Dex. This suggests DPSCs extract the same surface information. Surprisingly, the SEM images (Figure 3.5) show that in the absence of Dex, DPSCs from thin(-) produced calcium carbonates, whereas DPSCs from thin(+), thick(+) and TCP(+) produced both calcium phosphates and calcium carbonates. In cultures incubated

with Dex, DPSCs from all surfaces produced calcium phosphates, except for cells from thin(-) where mixture of calcium phosphates and calcium carbonates were found. These results suggest two things: when chemical inducer, Dex, was provided throughout the incubation period, DPSCs maintained normal biomineralization (calcium phosphates) even though surfaces were altered; when DPSCs were induced by the mechanical cues, calcium carbonate is deposited independent of chemical cues (Dex).

Third, the "double education" was also performed in the case of thin(-), where DPSCs first cultured on thin(-) for 21 days were transfered to thick(-) for 21 days incubation and then transfered back to thin(-) and thick(-) for another 21 days. The purpose of double education was to determine how DPSCs would respond when mechanical cues were reapplied. In Figure 3.6, confocal images show low cell densities on both thin(-) and thick(-) which might have resulted from reduced proliferation following multiple passage. Cells on thin(-) had a rounded appearance similar to cells which were first induced by mechanical cues, whereas the cells on thick(-) had a more extended appearance similar to DPSCs on thick(-) before education. The results imply that DPSCs might revert to their phenotypes expressed before education. As shown in Figure 3.7, SEM images show that double educated DPSCs on thin(-)produced calcium phosphates and the amounts of deposits were more than those found before education. On the other hand, only calcium carbonates deposits were detected on double educated DPSCs on thick(-), which remains the same deposits as educated thin(-) in the absence of Dex. These results suggest that in the case of removal of mechanical cue, DPSCs revert back to normal biomineralize (calcium phosphate) when mechanical cues are reintroduced. The results also suggest that mechanical cues are crucial in the pathway of biomineralization. The overall results lead us to conclude that even immunofluorescent staining analyses show that cells in direct

contact with surfaces (mechanical inducer) is not necessary to induce OCN expression in the upper cell layers, mechanical inducer still needs to present to maintain DPSCs biomineralization.

3.2 The effects of heterogeneous surface on DPSCs biomineralization

DPSCs differentiation has been studied by altering the mechanics of homogeneous PB surfaces and by the removal of mechanical and chemical cues. The results show that mechanical cue from hard PB and chemical cue from Dex can trigger DPSC biomineralization and the normal biomineralization will be interrupted if mechanical cue was removed. Here we discuss how DPSCs would behave when both hard and soft PB surface are present by spin-casting PB on micro and nano size imprinted patterned Si wafers.

The micro size of imprinted Si wafer was made by lithography as shown in Figure 3.8. The Si wafers were spun-cast hexamethyldisilazane (HMDS), which can improve the adherence of photoresist on Si wafers. The photoresist S1811 was further spun-cast on Si wafers and they were baked on 95˚C for 20 min. UV mask aligner – Karl uss MJB-3 was used to imprinted the pattern from mask onto photoresist. The Si wafers were further etched by Reactive Ion Etcher (RIE) –Trion Phantom III to imprint the pattern onto Si wafers. The residue photoresist was removed by the developer MF 312. PB was further spun-cast on imprinted Si wafers to cover the pattern surface to make thickness of 500Å (hard) and 1500Å (soft) area as Figure 3.9 shown. It has been shown that the confinement effects can dominate the polymer liquid structure factor and the surface spreading dynamics, which together strongly impact on the propagation of substrate roughness in thin homopolymer film coatings [48]. The AJR microscopic theory for χ (q,l) of simple liquids, in the Deryagin approximation, yields the prediction [49, 50]. For a discrete system the wave vector is $q_m = 2mp/d$ where d is the grating spacing and m is an integer. It has

also been shown when m is from 0 to 4, the major influence is from m=0 [1]. In our case of patterned surfaces, square patterned surfaces make the polymer film easily attenuation and then reach the uniform films.

The nano size of imprinted Si wafer was made by ion etching the PS/PMMA blend polymer mask. Two different ratio of PS/PMMA blending solution, 25/75 and 50/50, were used to spin-cast on Si wafers. Due to the phase separation, the patterned mask was made spontaneously [51, 52, 53, 54, 55]. Ion Milling (Gatan 600 CTMP Turbo Pumped Argon/Reactive Plasma DuoMill Dual Station Ion) was used to sputter the surfaces to imprint the pattern onto Si wafers. The residue polymer was further removed by melting at 700˚C. The patterned surfaces were analyzed by AFM as Figure 3.10 shown. DPSCs were cultured on these micro and nano size of patterned surfaces.

Laser scanning confocal microscopy was employed to investigate whether DPSCs sense the mechanical patterned surfaces after a 3 day incubation. The confocal images of DPSCs on micro size mechanical patterned surfaces are shown in Figure 3.11. It is very clear that DPSCs sense the mechanical patterned surfaces as actin filaments follow the underlying patterns. Similarly, the confocal images of DPSCs on nano size mechanical patterned surfaces (Figure 3.12) reveal that actin filaments also follow these underlying patterned areas. In comparison with DPSCs on non-patterned areas, actin filaments were well stretched and organized as DPSCs plated on flat PB films. The results from AFM and confocal images suggest that DPSCs can sense the micro and nano size of mechanical patterned surfaces and can further adjust their cytoskeletons to follow the underlying mechanical patterned areas.

Shear modulation force microcopy (SMFM) was also employed to investigate how DPSCs moduli change on mechanical patterned surfaces after 7 days incubation. Figure 3.13 shows the moduli of DPSCs on micro size mechanical patterned surfaces. The result shows that in the presence of Dex, DPSCs on different mechanical patterns have identical moduli. In the absence of Dex, moduli of DPSCs were found in two groups and the difference becomes apparent when pattern size becomes bigger. These results suggest that with the increase of patterned size, DPSCs can easily adhere completely on hard or soft areas instead of adhering partly on hard and soft areas which makes the mechanics of DPSCs fluctuate. On the other hand, Figure 3.14 shows the moduli of DPSCs on nano size mechanical patterned areas and non-patterned areas after 7 days incubation. The result shows that with the presence of Dex, no significant difference of DPSC moduli was found on patterned and non-patterned areas. However, in the absence of Dex, the moduli of DPSCs on non-patterned areas were smaller than those on patterned areas. These results suggest that DPSCs become harder on nano size mechanical patterned without Dex presents. All results are consistent with the conclusion that when DPSCs sit on a larger patterned area they can sit completely on a homogeneous area (hard or soft areas) where they can completely adjust their mechanics. In samples having large hard and soft areas, two groups of cells were identified, with distinct moduli indicating DPSCs adherence to hard and soft areas. However, when the patterned sizes decrease to certain sizes, DPSCs sit on heterogeneous areas (hard and soft areas) where they sense both hard and soft PB. However, in this case the mechanics of DPSCs is harder.

SEM/EDX was used to investigate whether DPSCs were triggered to biomineralize on micro and nano size of mechanical patterned surfaces after 21 days incubation. As shown in Figure 3.15, no biomineralization were found on micro size mechanical patterned surfaces

without Dex presents and very few deposits were found on those with Dex presents. The result shows that micro size of mechanical patterned surfaces cannot trigger DPSCs to biomineralize even with the presence of Dex. On the other hand, SEM images and EDX spectrum of DPSCs on nano size of mechanical patterned areas and non-patterned areas were shown on Figure 3.16. The result shows that biomineralization was found on both patterned and non-patterned areas when Dex presents and biomineralization were only found on patterned areas without the presence of Dex. The results suggest that nano size of mechanical patterned surfaces can trigger DPSCs to biomineralize. The overall results imply that the size of mechanical patterned surface plays a crucial rule on DPSCs biomineralization. When the size is too large, in this case is 5, 10μm and 5, 5μm, DPSCs can sense either hard or soft signal from surfaces and further adjust their mechanics to either hard or soft. However, no biomineralization was observed after a 21 day incubation which suggests that cells in contact with soft areas are preventing the DPSCs from biomineralizing and that they may also secrete factors which prevent other cells, which are in contact with hard areas, from biomineralizing. When the pattern size is intermediate, in this case is 3, 2μm, DPSCs sense both hard and soft surfaces and cause a failure of biomineralization by the competition of hard and soft signals from surfaces. However, when the pattern is nano sized, DPSCs sense both hard and soft signals from surfaces but are triggered to biomineralize.

This chapter described the effects of mechanical inducer on DPSCs biomineralization. To achieve this study, two different approaches were employed. First, DPSCs were tested for their ability to biomineralize when mechanical cues were altered by plating cells on thin PB, thick PB and TCP with and without Dex. After a 21 days incubation, cells were trypsinized and re-plated on thick PB, which does not induce DPSC differentiation, with and without Dex. After other 21 day incubation, LSCM and SEM/EDX were used to analyze the biomineralization. The

results showed that normal biomineralization (calcium phosphates) remains when Dex is present throughout the incubation period. The results also show that once DPSCs are induced by a mechanical cue, the cue needs to be present during incubation to maintain normal biomineralization (calcium phosphates). If the cue is removed, DPSCs promote the deposition of calcium carbonates and when the cue is reintroduced, DPSCs biomineralization normally. Secondly, DPSCs were tested for biomineralization when different mechanical cues are present together by plating DPSCs on mechanical patterned surfaces. The results showed that DPSC biomineralization strongly correlated to the size of mechanical pattern. In the case of micro size, cells adjust their mechanics to respond to multiple surface mechanics resulting in a failure to biomineralize. In the case of nano size patterns, cells still sensed the underlying patterned surfaces as hard and biomineralized suggesting that biomineralization was linked to the size of mechanical pattern. The overall results imply that the mechanical cues, hard PB, are not only the beginning key to trigger the pathway of DPSC biomineralizaton but also a participant factor to maintain the DPSC biomineralization on the pathway.

3.3 References

[48] Li Z, Tolan M, Hohr T, Kharas D, Qu S, Sokolov J, Rafailovich M, Lorenz H, Kotthaus JP, Wang J, Sinha SK, Gibaud A. Marcomolecules 1998; 31: 1915-1920

[49] Andelman D, Joanny JF, Robbins MO. Europhys. Lett. 1988; 7: 731

[50] Robbins MO, Andelman D, Joanny JF. Physical Review A 1991; 43(8): 4344-4354

[51] Liu Y, Quinn J, Rafailovich M, Sokolov J. Marcomolecules 1995; 28: 6347-6348

[52] Meiners JC, Ritzi A, Rafailovich M, Sokolov J, Mlynek J, Krausch G. App. Phys. A 1995; 61: 519-524

[53] Clarke CJ, Eisenberg A, La Scala J, Rafailovich M, Sokolov J, Li Z, Qu S. Marcomolecules 1997; 30: 4184-4188

[54] Cox J, Eisenberg A, Lennox R. Current Opinion in Colloid & Interface Science 1999; 4: 52-59

[55] Meli MV, Badia A, Grutter P, Lennox R. Nano Letters 2002; 2(2): 131-135

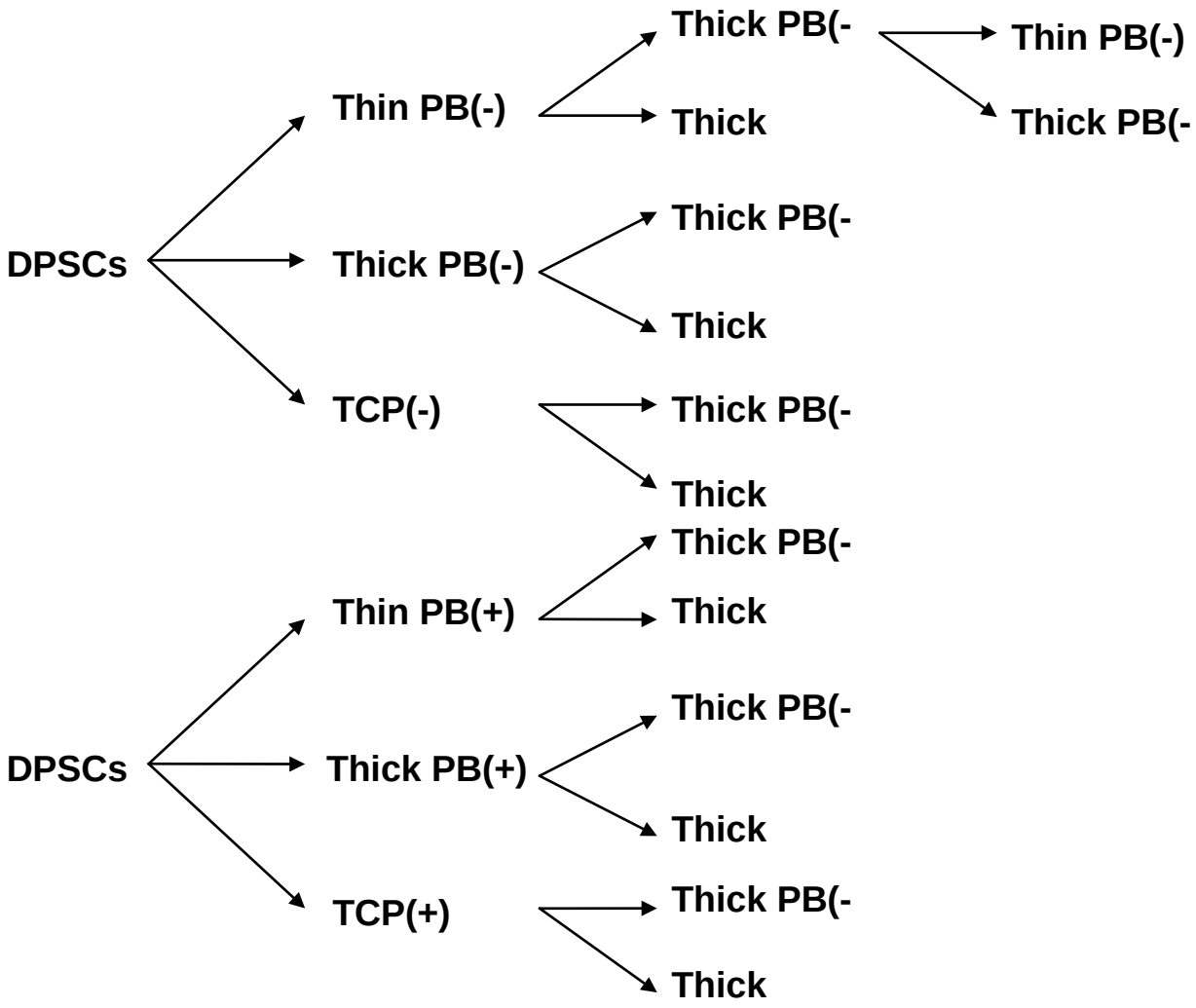

Figure 3.1 The experimental scheme of investigation of mechanical inducer on DPSC biomineralization.

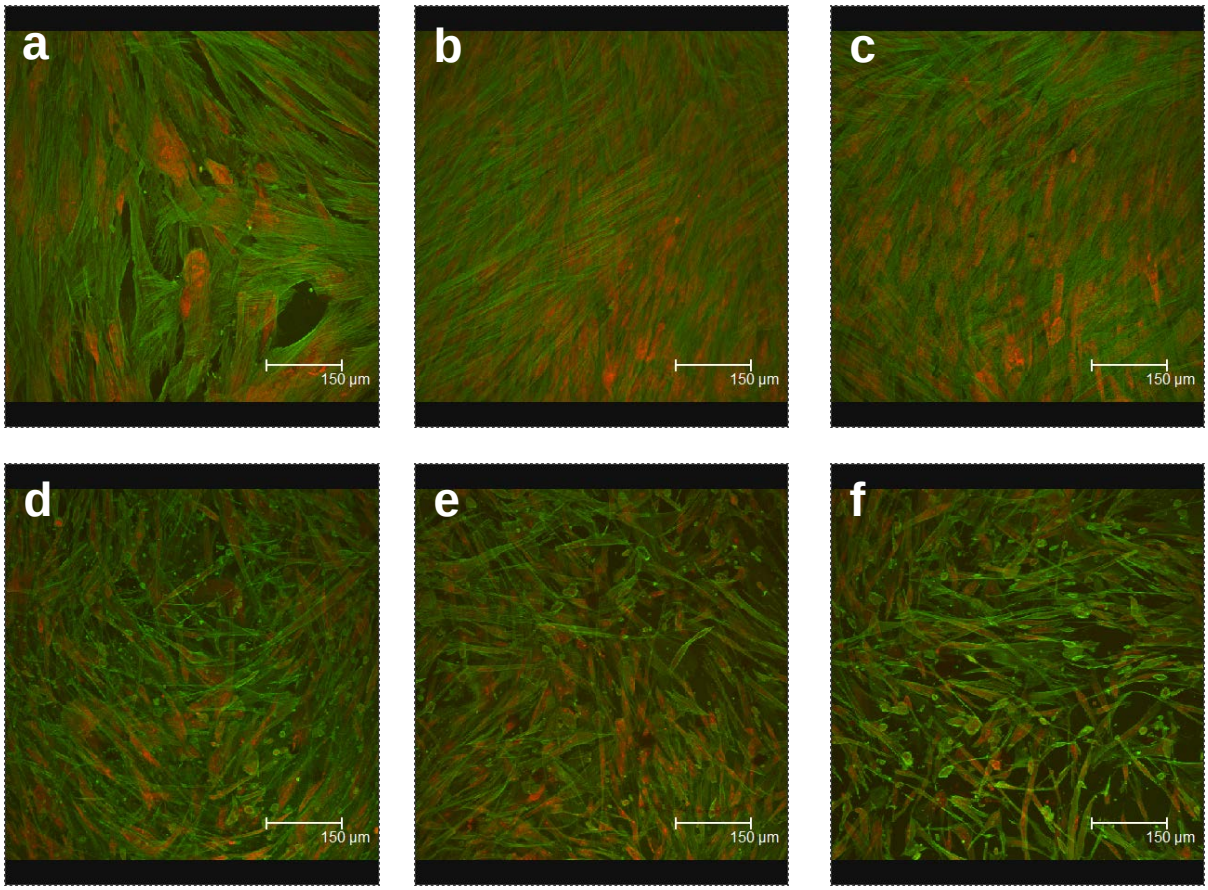

Figure 3.2 The confocal images of DPSCs on (a) thin PB, (b) thick PB and (c) TCP without the presence of Dex and those (c, d, e) with the presene of Dex.

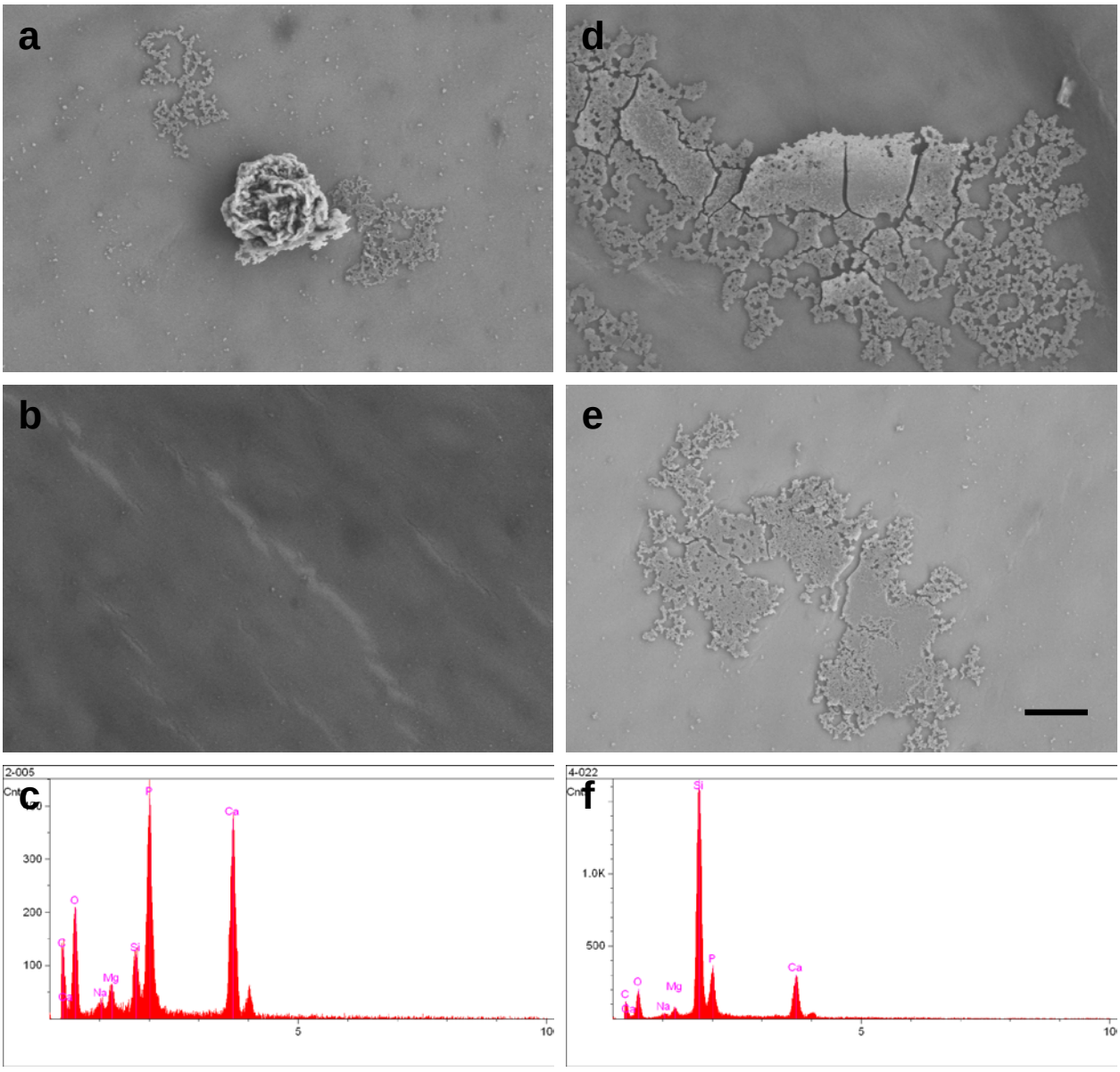

Figure 3.3 The SEM images of DPSCs on (a) thin PB and (b) thick PB without Dex presents and those (d, e) with Dex presents. The EDX spectrum of deposits on (c) thin PB and (f) thick PB showing the deposits are calcium phosphates. Scale bar= 40μm.

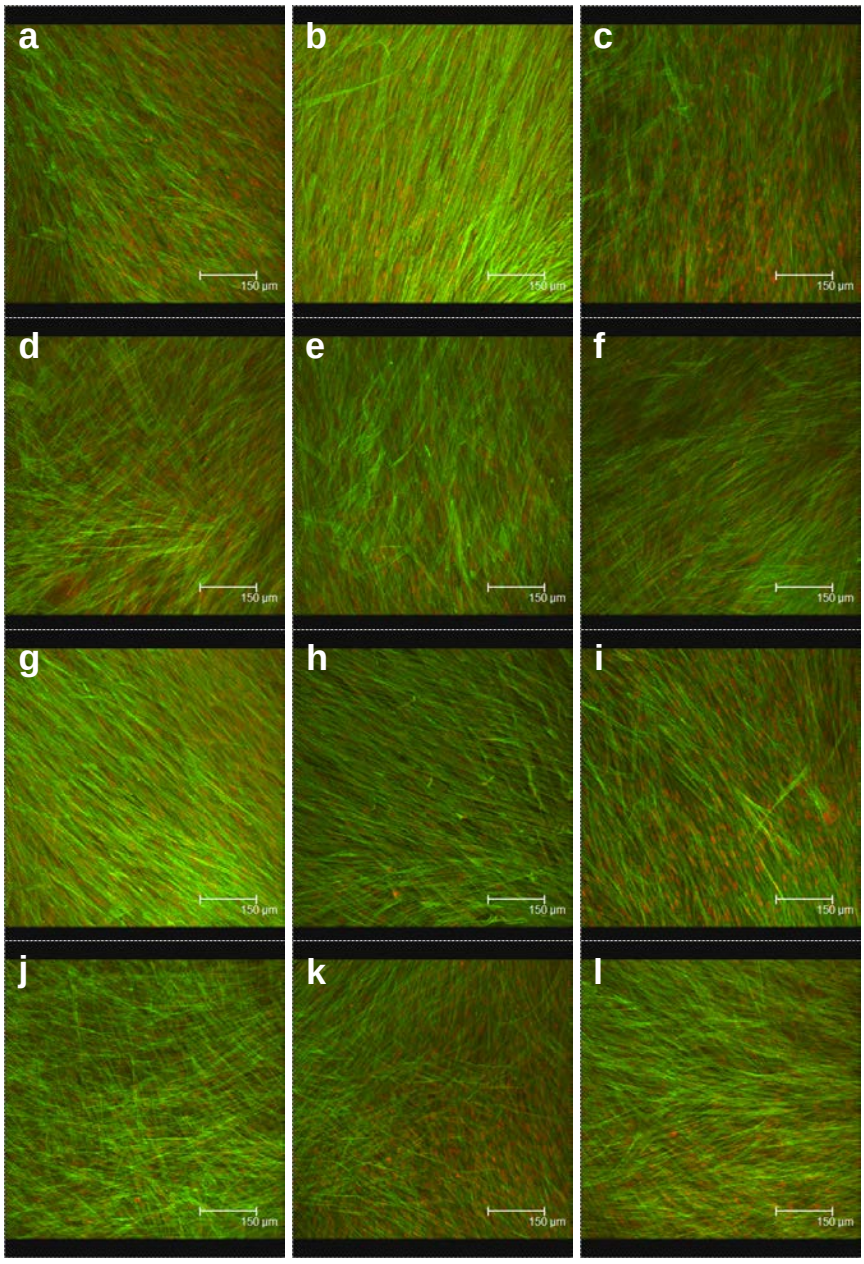

Figure 3.4 The confocal images of DPSCs after education from (a) thin PB(-), (b) thick PB(-), (c) TCP(-), (g) thin PB (+), (h) thick(+) and (i) TCP(+) without the presence of Dex and those (d, e, f, j, k, l) with the presence of Dex.

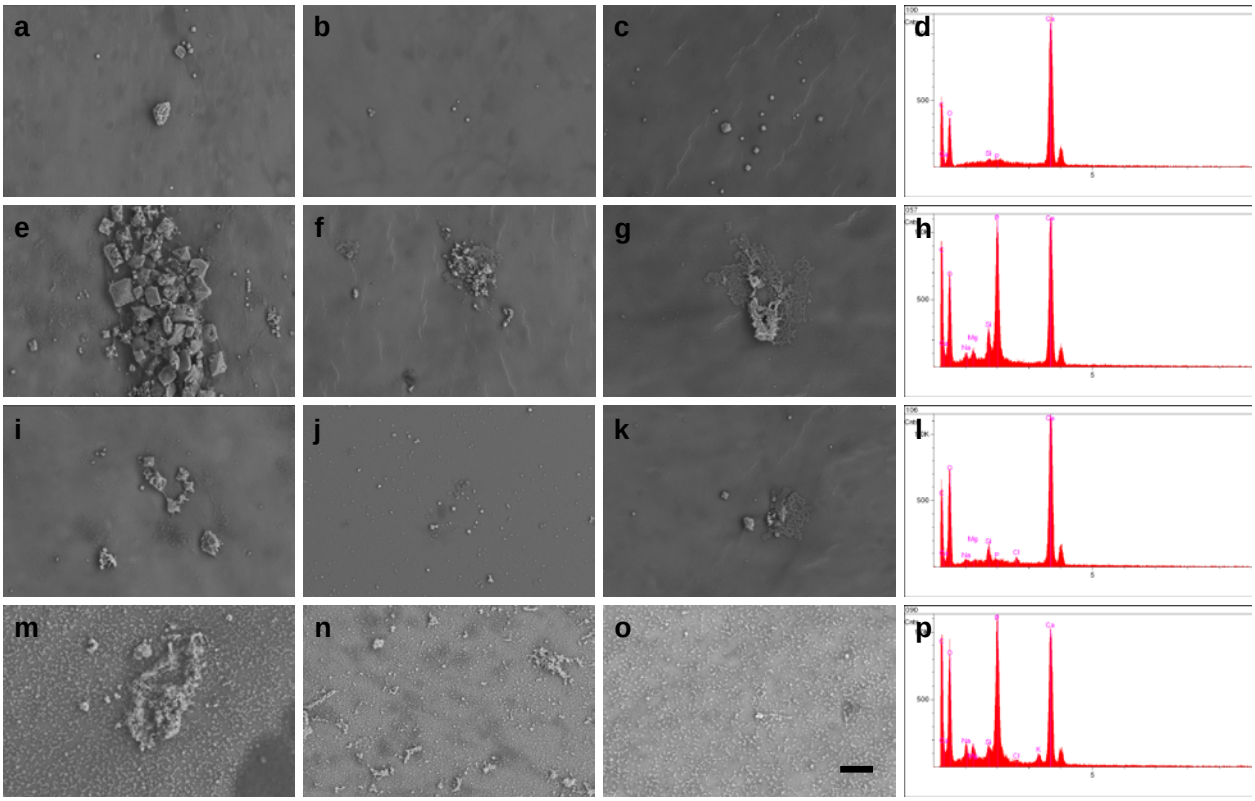

Figure 3.5 The SEM images of DPSCs after education from (a) thin PB(-), (b) thick PB(-), (c) TCP(-), (i) thin PB(+), (j) thick PB(+) and (k) TCP(+) without the presence of Dex and those (e, f, g, m, n, o) with the presence of Dex. The EDX spectrum (d, h, l, p) shows that deposits are calcium carbonates and calcium phosphates. Scale bar= 40μm.

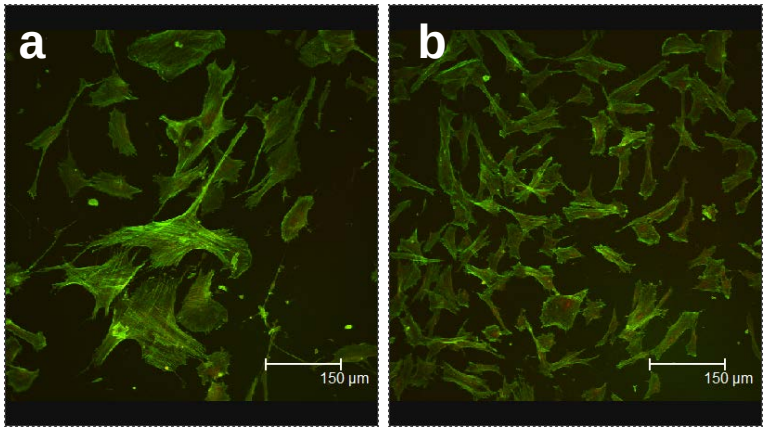

Figure 3.6 The confocal images of DPSCs after double education on (a) thin PB and (b) thick PB without the presence of Dex.

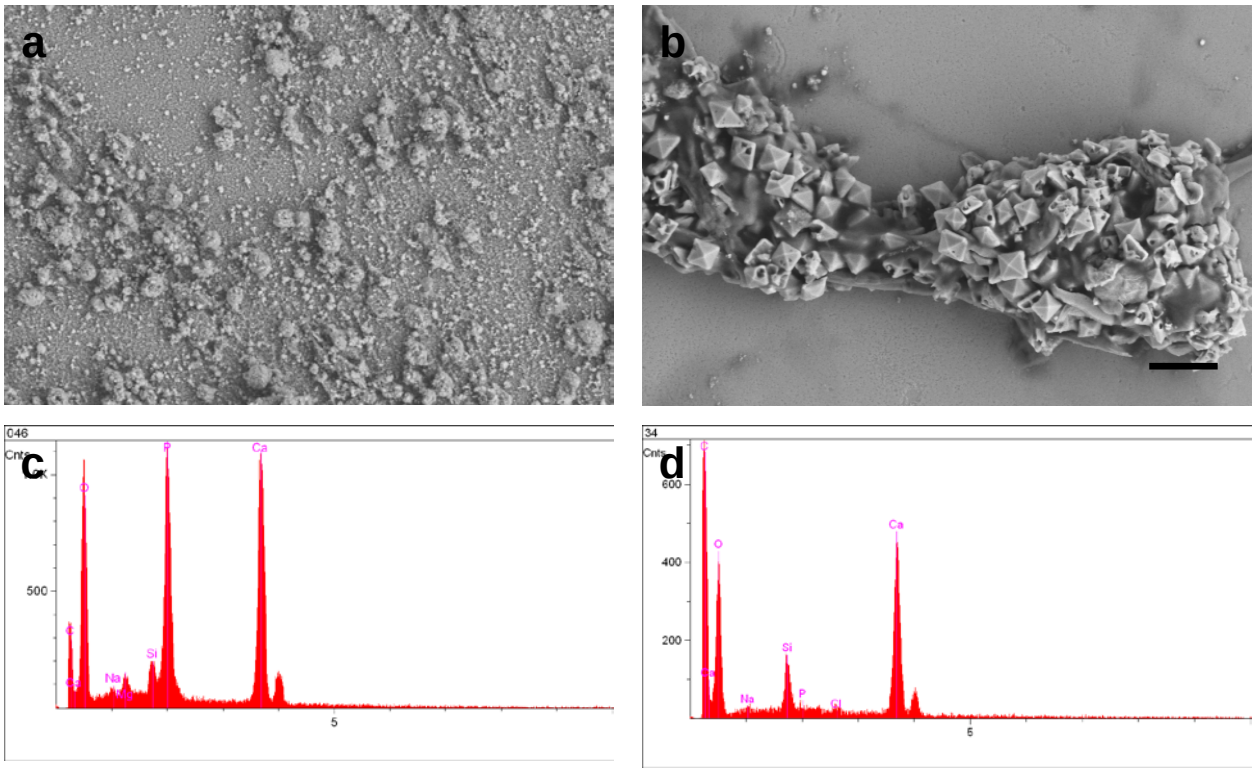

Figure 3.7 The SEM images of DPSCs after double education on (a) thin PB and (b) thick PB without the presence of Dex. The EDX spectrum of deposits on (c) thin PB and (d) thick PB showing the deposits are calcium carbonates and calcium phosphates. Scale bar= 40μm.

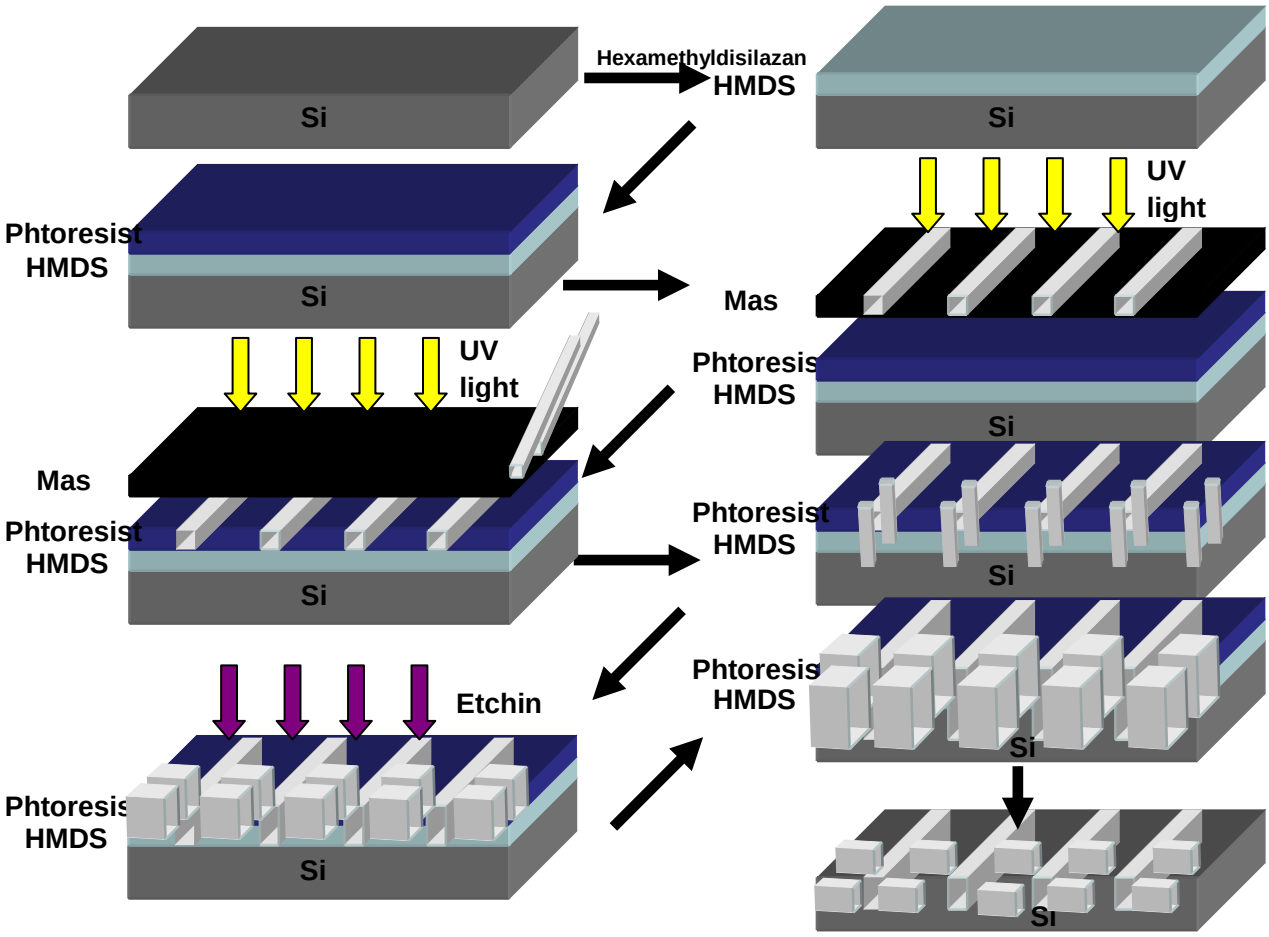

Figure 3.8 The experimental scheme of generating micro size imprinted pattern Si wafers by lithography.

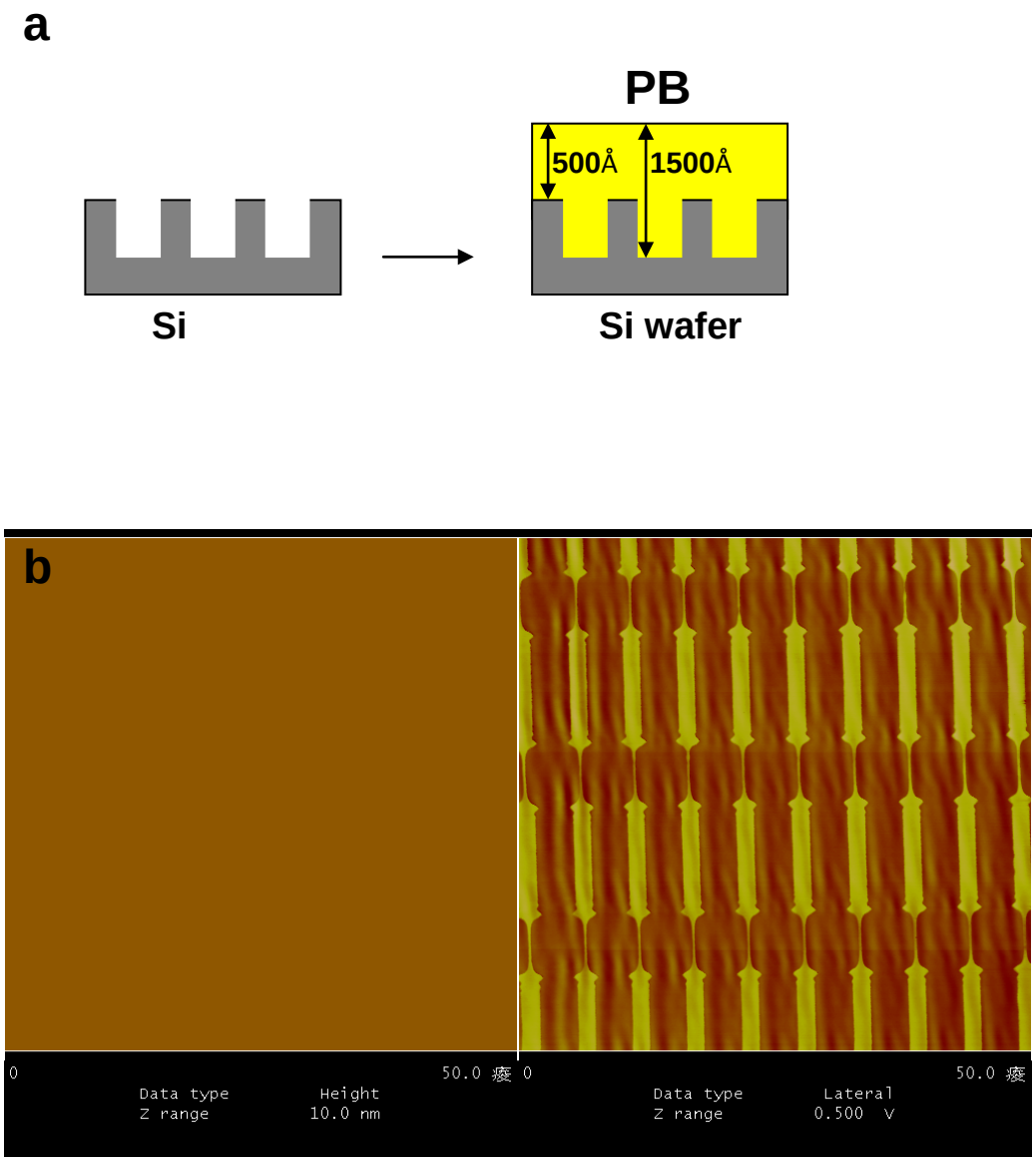

Figure 3.9 (a) The suggested mechanical patterned surface made by spin-casting PB to cover imprinted Si wafers with thickness of 500Å and 1500Å. (b) The AFM images shows flat topography (left side) and micro size mechanical pattern was produced (right side).

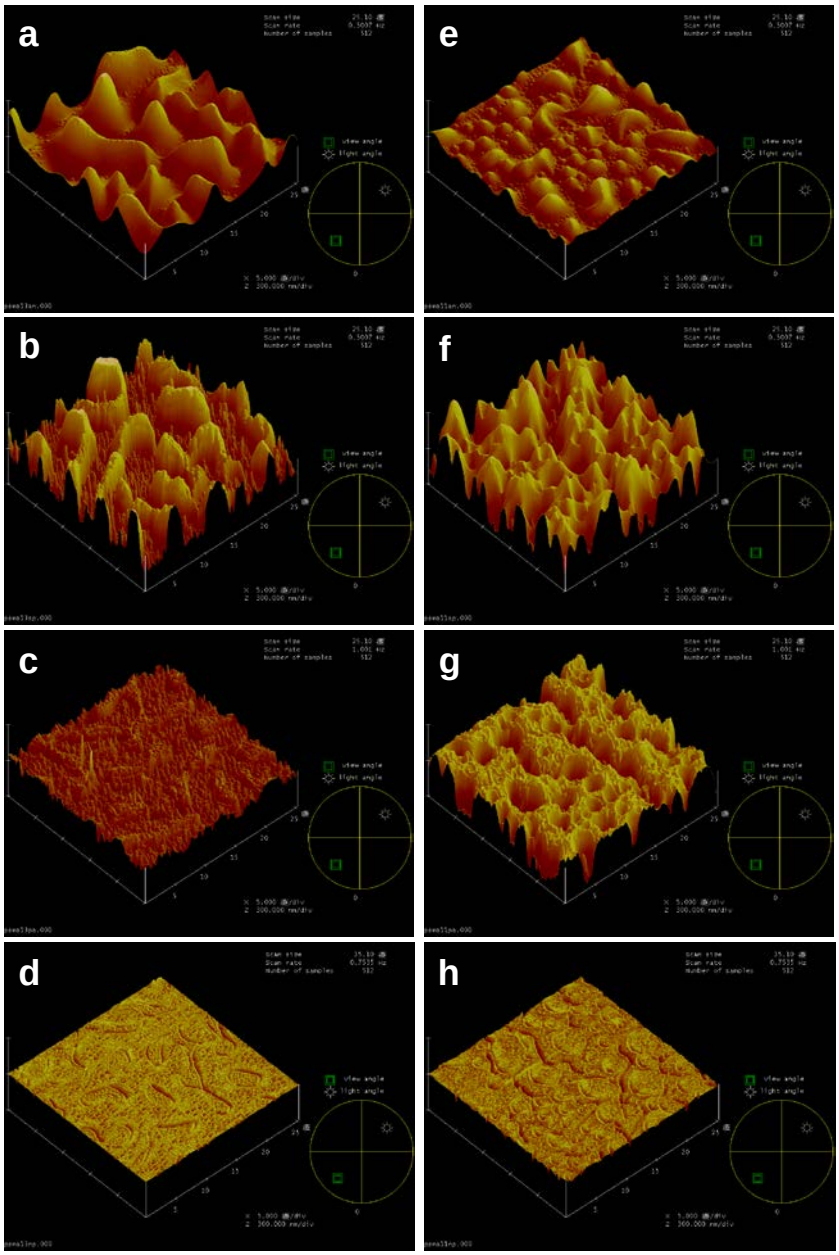

Figure 3.10 The AFM topography images of (a) spun-cast PS/PMMA, (b) after ion etching, (c) after removing residue polymer and (d) after spin-casting PB in the ratio of 25/75 and those (e, f, g, h) in the ratio of 50/50.

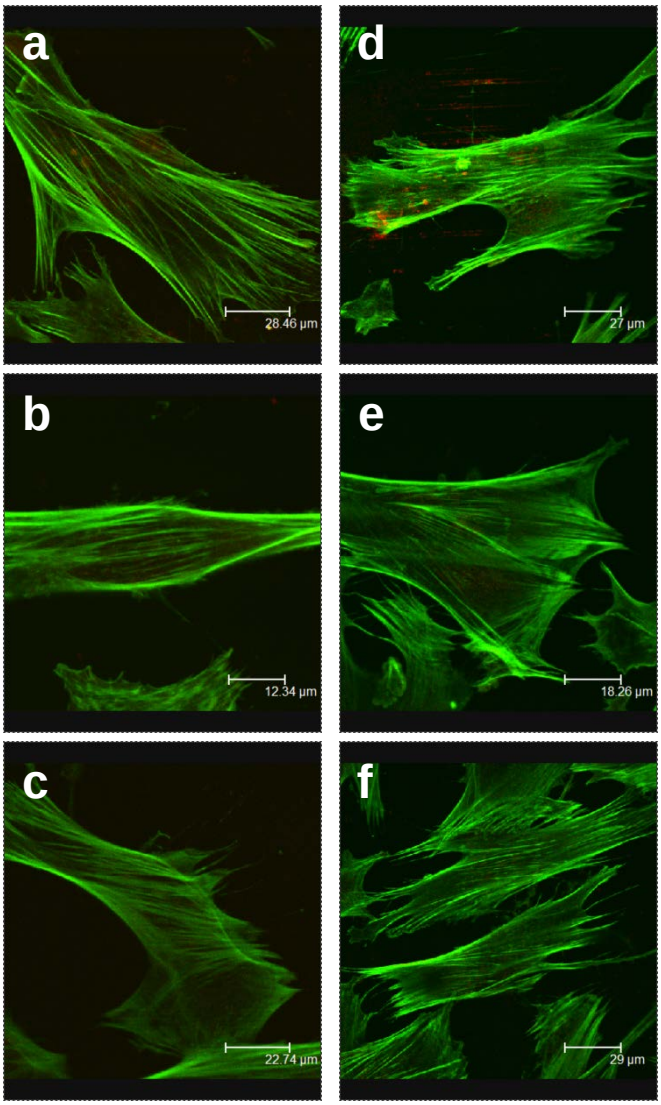

Figure 3.11 The confocal images of DPSCs on micro size mechanical patterned surface with size of (a) 3, 2µm, (b) 5, 5µm and (c) 5, 10µm with the absence of Dex and those (d, e, f) with the presence of Dex.

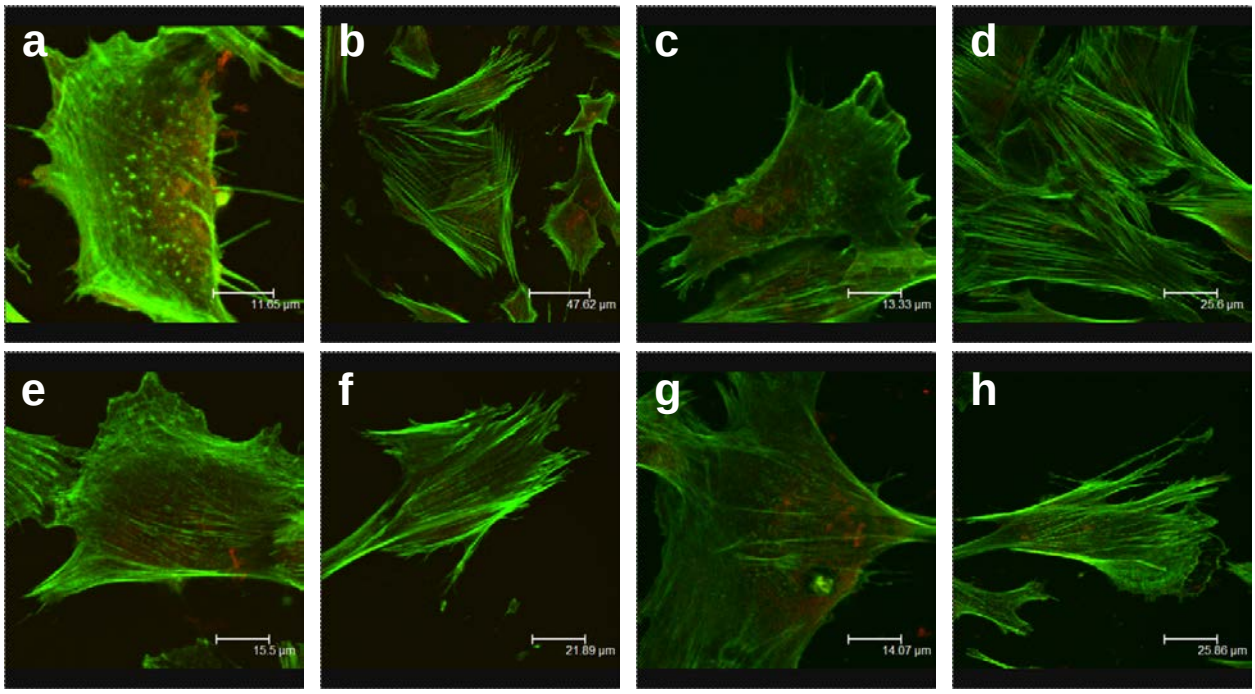

Figure 3.12 The confocal images of DPSCs on nano size (a) patterned area and (b) non-patterned area without the presence of Dex and (c) patterned area and (d) non-patterned area with the presence of Dex made by PS/PMMA in the ratio of 25/75. (e)~(h) are those made by PS/PMMA in the ratio of 50/50.

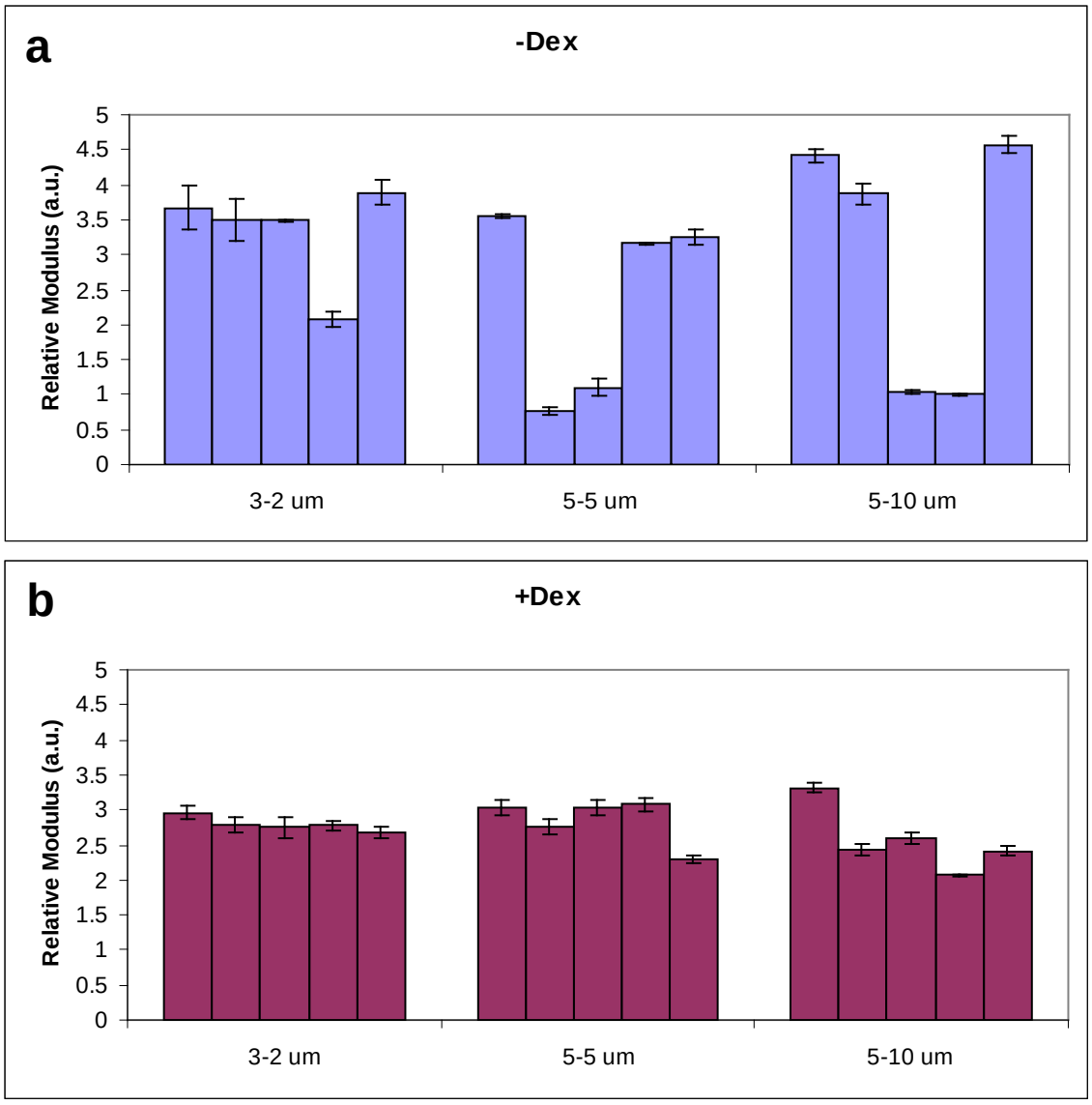

Figure 3.13 The moduli of DPSCs on different micro size of mechanical patterned surface (a) without Dex and (b) with Dex.

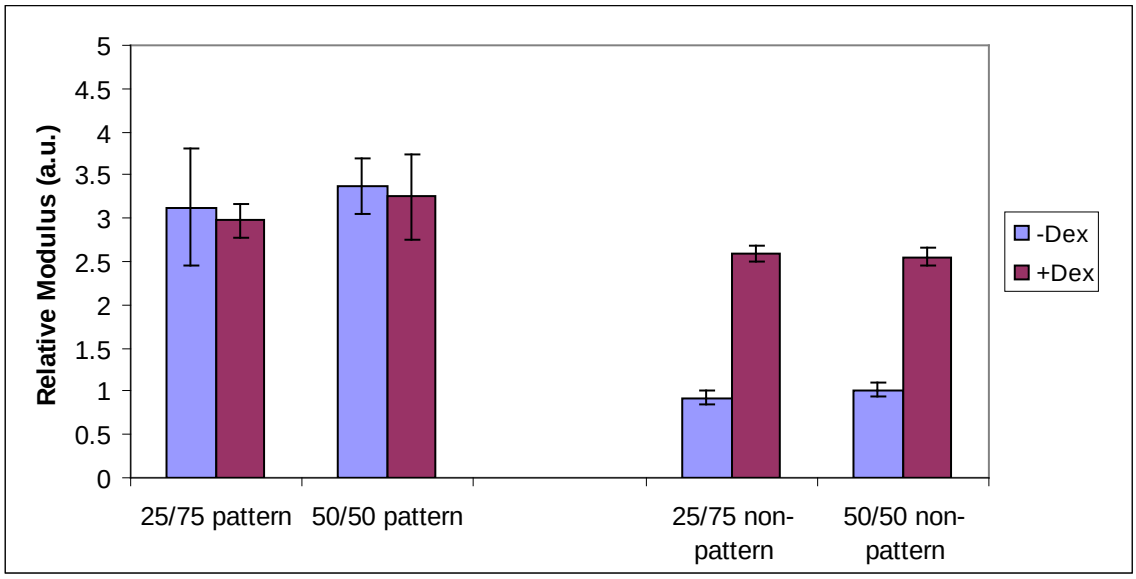

Figure 3.14 The moduli of DPSCs on nano size mechanical patterned and non-patterned areas made by different ratio of PS/PMMA with and without Dex.

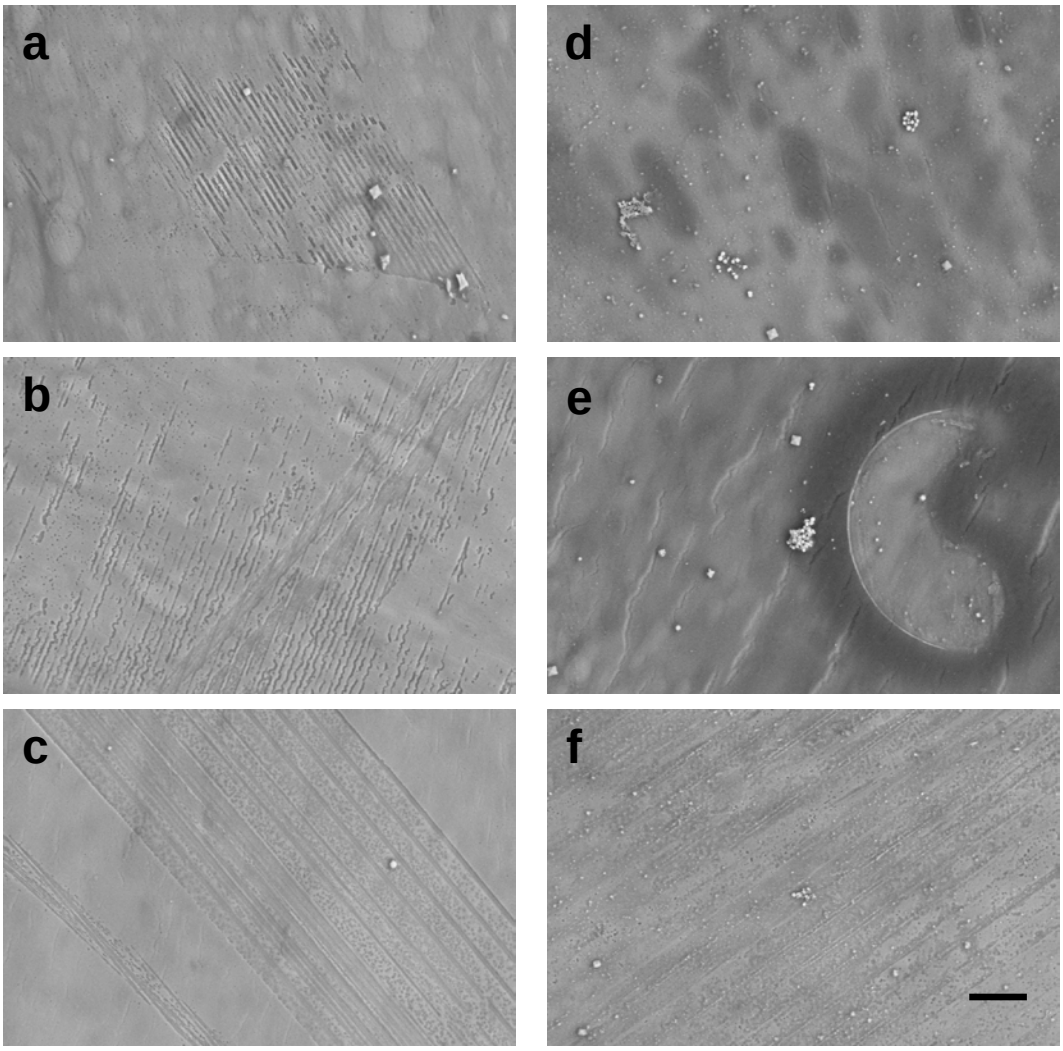

Figure 3.15 The SEM images of DPSCs grown on mechanical patterned with size of (a) 3, 2μm, (b) 5, 5μm and (c) 5, 10μm without the presence of Dex and those (d, e, f) with the presence of Dex after 21 days incubation. Scale Bar= 40μm.

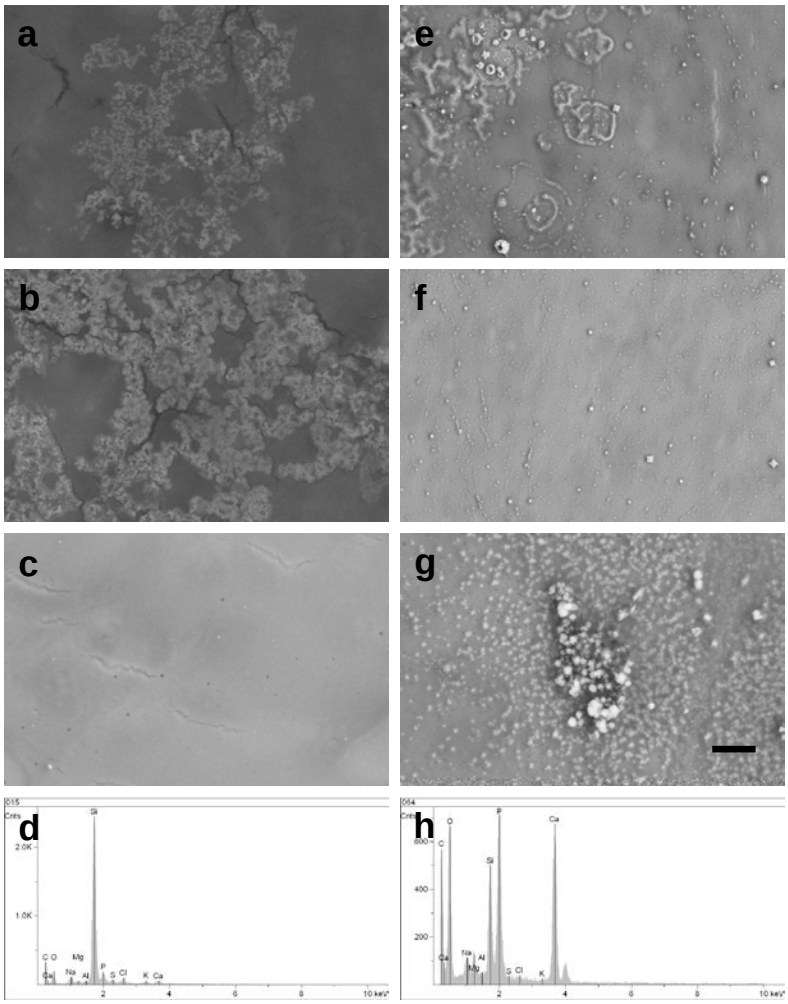

Figure 3.16 The SEM images of DPSCs grown on nano size mechanical patterned area made by (a) 25/75 ratio of PS/PMMA, (b) 50/50 ratio of PS/PMMA and (c) non-patterned area without presence of Dex and those (e, f, g) with the presence of Dex. The EDX spectrum (d) and (h) shows that the deposits are both calcium phosphates without and with Dex presents. Scal bar= 40μm.

References

[1] Lim CT, Zhou EH, Quek ST. Journal of Biomechanics 2006; 39: 195-216

[2] Chen CS, Mrksich M, Huang S, Whitesides GM, Ingber DE. Sciene 1997; 276(5317): 1425-1428

[3] Boudreau N, Bissell MJ. Current Opinion in Ccell Biology 1998 ; 10: 640-646

[4] Schwartz MA, Ginsberg MH. Nature Cell Biology 2002; 4: 65-68

[5] Nagayama K, Nagano Y, Sato M, Matsumoto T. Journal of Biomechanics 2006; 39(2): 293-301

[6] Zahalak GI, Wagenseil JE, Wakatsuki T, Elson EL. Biophysical Journal 2000; 79(5): 2369-2381

[7] Guilak F, Mow VC. Journal of Biomechanics 2000; 33(12): 1663-1673

[8] Engler AJ, Sen S, Sweeney HL, Discher DE. Cell 2006; 126: 677-689

[9] Holle AW, Engler AJ. Current Opinion in Biotechnology 2011; 22: 648-654

[10] Ingber DE. Ann. Med. 2003; 35: 564-577

[11] Lee G, Lim CT. TRENDS in Biotechnology 2006; 25(3): 111-118

[12] Vliet KJ, Bao G, Sureah S. Acta Materialia 2003; 51: 5881-5905

[13] Lim CT, Zhou EH, Li A, Vedula SRK, Fu HX. Materials Science an Engineering C. 2006; 26: 1278-1288

[14] Holle AW, Engler AJ. Current Opinion in Biotechnology 2011; 22: 648-654

[15] Engler AJ, Sen S, Sweeney HL, Discher DE. Cell 22006; 126: 677-689

[16] Engler AJ, Sweeney HL, Discher DE, Schwarzbauer JE. J. Musculoskelet Neuronal Interact 2007; 7(4): 335

[17] Discher DE, Janmey P, Wang YL. Sciene 2005 ; 310 : 1139-1143

[18] Rehfeldt F, Engler AJ, Eckhardt A, Ahmed F, Discher DE. Advanced Drug Delivery Reviews 2007; 59: 1329-1339

[19] Yeung T, Georges PC, Flanagan LA, Marg B, Ortiz M, Zahir N, Ming W, Weaver V, Janmey PA. Cell Motility and the Cytoskeleton 2005; 60: 24-34

[20] Sen S, Engler AJ, Discher DE. Cellular and Molecular Bioengineering 2009; 2(1): 39-48

[21] Reilly GC, Engler AJ. J. Biomechanics 2010; 43: 55-62

[22] Holle AW, Engler AJ. Nature Materials 2010: 9: 4-6

[23] Tse JR, Engler AJ. PLos ONE 2011; 6(1): e15978

[24] Gronthos S, Mankani M, Brahim J, Robey PG, Shi S. Proc. Natl. Acad. Sci. 2009; 97(25): 13625-13630.

[25] Almushayt A, Narayanan K, Zaki AE, George A. Gene Therapy 2006; 13: 611-620

[26] Gronthos S, Brahim J, Li W, Fisher LW, Cherman N, Boyde A, DeenBesten P, Robey PG, Shi S. J. Dental Research 2002; 811(8): 531-535

[27] Miura M, Gronthos S, Zhao M, Lu B, Fischer LW, Robeey PG, Shi S. Proc. Natl. Acad. Sci. 2003; 100(10): 5807-5812

[28] Nosrat IV, Smith CA, Mullally P, Olson L, Nosrat CA. European Journal of Neuroscience 2004; 19: 2388-2398

[29] Batouli S, Miura M, Brahim J, Tsutsui TW, Fischer LW, Gronthos S, Robey PG, Shi S. J. Dental Research 2003; 82(12): 976-981

[30] Shi S, Robey PG, Gronthos S. Bone 2001; 29(6): 531-539

[31] Cooper PR, Takahashi Y, Graham LW, Simon S, Imazato S, Smith AJ. J. Dent. 2010; 38: 687-697

[32] Goldberg M, Farges JC, Lacerd-Pinheiro S, et al. Pharmacol Res. 2008; 58: 137-147

[33] Li C, Koga T, Li C, Jiang J, Sharma S, Narayanan S, Lurio LB, Hu X, Jiao X, Sinha SK, Billet S, Sosnowik D, Kim H, Sokolov JC, Rafailovich M. Macromolecules 2005; 38: 5144-5151

[34] Zheng X, Rafailovich M, Sokolov J, Strzheemechny Y, Schwarz SA, Sauer BB, Rubinstein M. Physical Review Letters 1997; 79(2): 241-244

[35] Zhao W, Rafailovich M, Sokolov J, Fetters LJ, Plano R, Sanyal MK, Sinha SK, Sauer BB. Physical Review Letters 1993; 70(10): 1453-1456

[36] Tolan M, Seeck OH, Schlomka JP, Press W, Wang J, Sinha SK, Li Z, Rafailovich M, Sokolov J. Physical Review Letters 1998; 81(13): 2731-2734

[37] Ge S, Pu Y, Zhang W. Rafailovich M, Sokolov J. Physical Review Letters 22000; 85(11): 2340-2343

[38] Pu Y, Ge S, Rafailovich M, Sokolov J, Duan Y, Pearce E, Zaitsev V, Schwarz S. Langmuir 2001; 17: 5865-5871

[39] Koo J, Rafailovich M, Medved L, Tsurupa G, Kudryk BJ, Liu Y, Galanakis DK. J. Thromb Haemost 2010; 8: 2727-2734

[40] Oliver WC, Pharr GM. J. Materials Res. 1992; 7(6): 1564-1583

[41] Ghosh K, Pan Z, Guan E, Ge S, Liu Y, Nakamura T, Ren XD, Rafailovich M, Clark RAF. Biomaterials 2007; 28: 671-679

[42] Ingber DE, Heidemann SR, Lamoureux P, Buxbaum RE. J. Applied Physiology 2000; 89: 1663-1678

[43] Yeung T, Georges PC, Flanagan LA, Marg B, Ortiz M, Funaki M, Zahir N, Ming W, Weaver V, Janmery PA. Cell Motility and the Cytoskeeleton 2005; 6: 24-34

[44] Ba X, Hadijiargyrou M, DiMasi E, Meng Y, Simon M, Tan Z, Rafailovich M. Biomaterials 2011 ; 32 : 7831-7838

[45] Meng Y, Qin Y, Dimasi E, Ba X, Rafailovich M, Pernodet N. Tissue Engineering: Part A 2009 ; 15(2) : 355-366

[46] Canalis E. J. Clinical Endocrinology and Metabolism 81: 3441-3447

[47] Mei-Fway I, Hiroshi K, Hideaki S, Junko N, Toshitsugu S, Kazuo C. J. Endocrinology 2005; 185: 131-138

[48] Li Z, Tolan M, Hohr T, Kharas D, Qu S, Sokolov J, Rafailovich M, Lorenz H, Kotthaus JP, Wang J, Sinha SK, Gibaud A. Marcomolecules 1998; 31: 1915-1920

[49] Andelman D, Joanny JF, Robbins MO. Europhys. Lett. 1988; 7: 731

[50] Robbins MO, Andelman D, Joanny JF. Physical Review A 1991; 43(8): 4344-4354

[51] Liu Y, Quinn J, Rafailovich M, Sokolov J. Marcomolecules 1995; 28: 6347-6348

[52] Meiners JC, Ritzi A, Rafailovich M, Sokolov J, Mlynek J, Krausch G. App. Phys. A 1995; 61, 519-524

[53] Clarke CJ, Eisenberg A, La Scala J, Rafailovich M, Sokolov J, Li Z, Qu S. Marcomolecules 1997; 30, 4181-4188

[54] Cox J, Eisenberg A, Lennox R. Current Opinion in Colloid & Interface Science 1999; 4: 52-59

[55] Meli MV, Badia A, Grutter P, Lennox R. Nano Letters 2002; 2(2): 131-135